

**Influence of nonmagnetic impurity scattering on spin dynamics in diluted magnetic semiconductors**M. Cygorek,<sup>1</sup> F. Ungar,<sup>1</sup> P. I. Tamborenea,<sup>2</sup> and V. M. Axt<sup>1</sup><sup>1</sup>*Theoretische Physik III, Universität Bayreuth, 95440 Bayreuth, Germany*<sup>2</sup>*Departamento de Física and IFIBA, FCEN, Universidad de Buenos Aires, Ciudad Universitaria, Pabellón I, 1428 Ciudad de Buenos Aires, Argentina*

(Received 9 September 2016; revised manuscript received 29 November 2016; published 13 January 2017)

The doping of semiconductors with magnetic impurities gives rise not only to a spin-spin interaction between quasifree carriers and magnetic impurities but also to a local spin-independent disorder potential for the carriers. Based on a quantum kinetic theory for the carrier and impurity density matrices as well as the magnetic and nonmagnetic carrier-impurity correlations, the influence of the nonmagnetic scattering potential on the spin dynamics in DMS after optical excitation with circularly polarized light is investigated using the example of Mn-doped CdTe. It is shown that non-Markovian effects, which are predicted in calculations where only the magnetic carrier-impurity interaction is accounted for, can be strongly suppressed in the presence of nonmagnetic impurity scattering. This effect can be traced back to a significant redistribution of carriers in  $\mathbf{k}$ -space which is enabled by the build-up of large carrier-impurity correlation energies. A comparison with the Markov limit of the quantum kinetic theory shows that, in the presence of an external magnetic field parallel to the initial carrier polarization, the asymptotic value of the spin polarization at long times is significantly different in the quantum kinetic and the Markovian calculations. This effect can also be attributed to the formation of strong correlations, which invalidates the semiclassical Markovian picture and it is stronger when the nonmagnetic carrier-impurity interaction is accounted for. In an external magnetic field perpendicular to the initial carrier spin, the correlations are also responsible for a renormalization of the carrier spin precession frequency. Considering only the magnetic carrier-impurity interaction, a significant renormalization is predicted for a very limited set of material parameters and excitation conditions. Accounting also for the nonmagnetic interaction, a relevant renormalization of the precession frequency is found to be more ubiquitous.

DOI: [10.1103/PhysRevB.95.045204](https://doi.org/10.1103/PhysRevB.95.045204)**I. INTRODUCTION**

Most of the devices based on the spintronics paradigm that are commercially available today use the fact that spin-up and spin-down carriers exhibit different transmission and reflection probabilities at interfaces involving ferromagnetic metals [1,2]. However, some applications, like spin transistors [3], require the control not only of spin-up and spin-down occupations, but also of the coherent precession of spins perpendicular to the quantization axis provided by the structure. For this purpose, spintronic devices based on semiconductors are preferable to metallic structures since the dephasing time in a metal is about three orders of magnitude shorter than in a semiconductor [4]. In the context of semiconductor spintronics [5–7], a particularly interesting class of materials for future applications are diluted magnetic semiconductors (DMS) [8–22], which are obtained when semiconductors are doped with transition metal elements, such as Mn, which act as localized magnetic moments. While some types of DMS, such as  $\text{Ga}_{1-x}\text{Mn}_x\text{As}$ , exhibit a ferromagnetic phase [8,23], other types of DMS, like the usually paramagnetic  $\text{CdMnTe}$ , are especially valued for the enhancement of the effective carrier  $g$  factor by the giant Zeeman effect that can be used, e.g., to facilitate an injection of a spin-polarized current into a light-emitting diode [24].

A number of different aspects of DMS have been investigated in the past. These include the growth as well as structural and material properties of bulk DMS and DMS heterostructures (cf. review articles Refs. [8,25,26] and references therein), the magnetic order [27] and its control via ultrafast demagnetization after optical excitation [28–31], which is

particularly relevant for strongly  $p$ -doped DMS, or collective effects such as the formation of magnetic polarons [32–35] and spin waves [36,37]. Important insights into the fundamental spin physics in DMS can be obtained by investigating the spin dynamics in ultrafast optical pump-probe experiments [10,20,38,39]. For this purpose, intrinsic or  $n$ -doped DMS are particularly transparent because they are usually paramagnetic and, thus, the long-range magnetic order of the impurities, which complicates the analysis of the measured signals, is negligible.

In these systems, the spin dynamics is typically dominated by spin-flip scattering of quasifree carriers at the magnetic impurities, which leads to an exchange of spins between the carrier and impurity subsystems [22]. The exchange interaction responsible for the spin-flip scattering, which can be modeled by a Kondo-like Hamiltonian [40,41], has two distinct microscopic origins, the exchange part of the Coulomb interaction between carriers and impurities and a virtual hopping of quasifree carriers onto  $d$ -shell states of the magnetic impurities [42]. The contribution of the latter to the exchange interaction follows directly from a Schrieffer-Wolff transformation [43]. The same microscopic sources that yield the Kondo-like magnetic exchange interaction are also responsible for a nonmagnetic local interaction between carriers and impurities in the DMS. In  $\text{Cd}_{1-x}\text{Mn}_x\text{Te}$ , the nonmagnetic interaction ( $\sim 1.6$  eV [44]) is about one order of magnitude stronger than the magnetic interaction ( $\sim 220$  meV [45]). To understand why the nonmagnetic carrier-impurity interaction in  $\text{Cd}_{1-x}\text{Mn}_x\text{Te}$  is so strong, it is instructive to consider a model where electrons at unit cells without Mn atoms experience the band structure of CdTe and electrons at

unit cells where the Cd ions are replaced by Mn experience the band structure of MnTe. CdTe crystallizes in a zinc-blende structure, while the lowest energetic crystal structure of bulk MnTe is the NiAs structure [46]. Thus, when CdTe is doped with Mn impurities, the MnTe units are also forced into a zinc-blende structure. This leads to a large energy penalty with respect to its bulk form and, thus, to a significantly higher local conduction band edge than CdTe, which determines the strength of the effective nonmagnetic local carrier-impurity interaction.

Despite its strength, the nonmagnetic carrier-impurity interaction in DMS has been discussed in the literature, to the best of our knowledge, only in the context of transport problems [41], where it gives rise to an additional contribution to the resistance due to nonmagnetic impurity scattering, and for explaining shifts of the optical spectra of semiconductor structures upon doping with magnetic impurities [44]. The effects of nonmagnetic impurity scattering have, so far, not been addressed in the literature in the context of ultrafast spin dynamics in DMS. The reason for this is that the spin dynamics in DMS is almost always described by theoretical approaches that end up with Markovian rate equations for the spin transfer between quasifree carriers and impurities and other processes [19,22,30,31,47–52]. On the level of rate equations, the nonmagnetic impurity scattering of carriers at the impurities is an elastic process that conserves the spins of carriers and impurities individually and only leads to a redistribution of carriers to states with the same energy as before the scattering event. As a consequence, the carrier occupation and spin density remains unchanged by the nonmagnetic scattering in systems with a parabolic band structure and isotropic carrier distributions in  $\mathbf{k}$  space. Thus rate equations only predict an influence of nonmagnetic impurity scattering on the spin dynamics if, e.g.,  $\mathbf{k}$ -dependent effective fields due to spin-orbit coupling are present like in the Elliott-Yafet [53] or D'yakonov-Perel' [54] mechanisms. Although it is, in principle, possible to study DMS systems where the carrier spin dephasing in such effective fields competes with spin-flip scattering [55], this situation is not very common and, in this article, we focus on DMS with negligible spin-orbit interaction.

In recent studies based on a non-Markovian quantum kinetic theory [56] that did not account for nonmagnetic impurity scattering, it was predicted that in certain situations, such as confined systems like quantum wells and optical excitations close to the band edge [57], the spin dynamics in DMS after optical excitation deviates significantly from the Markovian exponential behavior. For example, the time evolution of the spin polarization can become nonmonotonic [58]. Furthermore, genuine many-body correlation effects, such as a renormalization of the carrier spin precession frequency and the build-up of correlation energy [59] may influence the ultrafast spin dynamics. The build-up of correlation energy was found to enable a scattering of electrons to states with higher kinetic energy and it affects, in particular, the asymptotic values of the carrier spin polarization in the presence of an external magnetic field at long times after the optical excitation [60]. Also, these many-body correlation effects cannot be explained in a theoretical description based on Markovian rate equations for uncorrelated carriers and impurities. Since the

appearance of non-Markovian behavior and correlation effects depends strongly on the dynamics of carriers in  $\mathbf{k}$  space, it can be expected that the strong nonmagnetic carrier-impurity interaction, which is present in real DMS but has not been included in the framework of the quantum kinetic theory [56] so far, significantly influences the non-Markovian spin dynamics.

The goal of the present paper is to investigate the influence of the nonmagnetic carrier-impurity interaction on the ultrafast electron spin dynamics in paramagnetic II-VI DMS after optical excitation. To this end, the quantum kinetic theory of Ref. [56] is extended and not only the magnetic  $s$ - $d$  interaction is taken into account, but also the nonmagnetic carrier-impurity interaction as well as Zeeman energies for carriers and impurities, which makes it possible to study the spin dynamics in the presence of an external magnetic field.

Here, we find that in the conduction band of a narrow  $\text{Cd}_{1-x}\text{Mn}_x\text{Te}$  quantum well, non-Markovian effects predicted by calculations neglecting the nonmagnetic carrier-impurity interaction are strongly suppressed by nonmagnetic impurity scattering. While, in this case, the nonmonotonic behavior of the spin dynamics disappears, the quantum kinetic theory predicts quantitative changes in the effective spin transfer rate compared with its Markovian value obtained by Fermi's golden rule. The suppression of the non-Markovian features is mainly caused by a significant redistribution of carriers away from the band edge where the non-Markovian effects are particularly strong [57]. This carrier redistribution is facilitated by the build-up of strong carrier-impurity correlations providing a correlation energy of the order of a few meV per electron that leads to an increase of the average kinetic electron energy by about the same amount. Due to the different strengths of the interactions in the conduction band of  $\text{Cd}_{1-x}\text{Mn}_x\text{Te}$ , the nonmagnetic carrier-impurity correlation energy is much larger than the magnetic correlation energy studied before in Ref. [59]. In other cases, such as in the valence band of  $\text{Cd}_{1-x}\text{Mn}_x\text{Te}$ , the nonmagnetic impurity scattering can be much weaker than the magnetic spin-flip scattering and the non-Markovian effects prevail. In the presence of an external magnetic field parallel to the initial carrier spin polarization, the correlation-induced change of the asymptotic value of the carrier spin polarization at long times  $t$  with respect to its mean field value [60] is found to be significantly enhanced when in addition to the magnetic carrier-impurity interaction also the nonmagnetic interaction is accounted for. If the initial carrier spin polarization is perpendicular to the external magnetic field, the carrier spins precess about the effective field comprised of the external field and the mean field due to the impurity magnetization. As shown in Ref. [59], the carrier-impurity correlations built up by the magnetic  $s$ - $d$  interaction renormalize the carrier spin precession frequency. Here, we show that when both, the magnetic and the nonmagnetic interactions are taken into account, the renormalization of the carrier spin precession frequency can be different in sign and magnitude compared with calculations in which only the magnetic interaction is considered.

The article is structured as follows: first, quantum kinetic equations of motion for the carrier and impurity density matrices as well as for the magnetic and nonmagnetic carrier-impurity correlations are formulated for a DMS with magnetic

and nonmagnetic carrier-impurity interactions. Then, we derive the Markov limit of the quantum kinetic theory which enables a comparison and allows us to distinguish the genuine quantum kinetic effects from the Markovian behavior. Furthermore, from the Markov limit we can derive analytic expressions for the carrier-impurity correlation energies as well as the correlation-induced renormalization of the carrier spin precession frequency. After having laid out the theory, we present numerical simulations of the quantum kinetic equations for the conduction band of a  $\text{Cd}_{1-x}\text{Mn}_x\text{Te}$  quantum well including magnetic and nonmagnetic scattering at the Mn impurities and discuss the energetic redistribution of carriers as well as the correlation energies. Then, we estimate the influence of nonmagnetic impurity interaction on the spin dynamics in the valence band of  $\text{Cd}_{1-x}\text{Mn}_x\text{Te}$ . Finally, we discuss the effects of the nonmagnetic impurity scattering on the spin dynamics in DMS in the presence of an external magnetic field parallel and perpendicular to an initial nonequilibrium carrier spin polarization.

## II. THEORY

### A. DMS Hamiltonian

In the present paper, we consider an intrinsic DMS such as  $\text{Cd}_{1-x}\text{Mn}_x\text{Te}$  in the presence of an external magnetic field. The effective magnetic  $s$ - $d$  exchange interaction between conduction band carriers and localized magnetic impurities is usually modeled by [41,45]

$$H_{\text{sd}} = J_{\text{sd}} \sum_{Ii} \hat{\mathbf{S}}_I \cdot \hat{\mathbf{s}}_i \delta(\mathbf{R}_I - \mathbf{r}_i), \quad (1a)$$

where  $\hat{\mathbf{S}}_I$  and  $\hat{\mathbf{s}}_i$  are the spin operators of the  $I$ th magnetic impurity and the  $i$ th conduction band electron, respectively, and  $\mathbf{R}_I$  and  $\mathbf{r}_i$  are the corresponding positions.  $J_{\text{sd}}$  is the magnetic coupling constant, which defines the strength of the magnetic carrier-impurity interaction. We assume that the nonmagnetic carrier-impurity interaction can be written similarly as

$$H_{\text{imp}} = J_0 \sum_{Ji} \delta(\mathbf{R}_J - \mathbf{r}_i), \quad (1b)$$

where  $J_0$  is the nonmagnetic coupling constant. In order to account for spin-independent scattering not only at Mn impurities but also at additional nonmagnetic scattering centers, such as in quaternary compound DMSs like  $\text{HgCdMnTe}$  [55], we allow the number of scattering centers  $N_{\text{imp}}$  in general to be larger than the number of magnetic impurities  $N_{\text{Mn}}$ . Here, we use the notation that the index  $I$  runs from 1 to  $N_{\text{Mn}}$  while the index  $J$  runs from 1 to  $N_{\text{imp}}$ . The value of the coupling constant for the magnetic impurity interaction in DMS is well established in the literature [45]. Here, we determine the value of the nonmagnetic carrier-impurity interaction so that the shifts of optical spectra upon doping of CdTe with Mn [44] are reproduced within the mean-field/virtual-crystal approximation of  $H_{\text{imp}}$ .

Note that we assume that the carrier-impurity interaction is short-range although it originates mainly from the Coulomb interaction between carriers and impurities. This assumption is justified for II-VI DMS, since the Mn impurities are

incorporated into the II-VI lattice isoelectrically. Thus the long-range monopole part of the Coulomb interaction between electrons and Mn impurities is the same as the corresponding part of the interaction between electrons and the Cd ions that are replaced by the Mn ions. Therefore the long-range part of the nonmagnetic Mn-carrier interaction is already covered by the effective crystal Hamiltonian, where Coulomb interactions are screened by the sea of electrons in the valence bands. The long-range part of the Coulomb interaction may be expected to be relevant in III-V DMS, where Mn ions typically act as acceptors and remain negatively charged [8]. However, even in the case of GaMnAs, models using a local approximation for the nonmagnetic carrier-impurity interaction have been successfully employed in the framework of the  $V$ - $J$  tight-binding model of Ref. [61], where a good quantitative agreement with *ab initio* calculations for the Curie temperature and with experimental data for the optical conductivity was obtained.

In second quantization and in  $\mathbf{k}$  space, the total Hamiltonian of the DMS system under consideration is

$$H = H_0 + H_{\text{sd}} + H_{\text{imp}} + H_Z^e + H_Z^{\text{Mn}}, \quad (2a)$$

$$H_0 = \sum_{\mathbf{k}\sigma} \hbar\omega_{\mathbf{k}} c_{\sigma\mathbf{k}}^\dagger c_{\sigma\mathbf{k}}, \quad (2b)$$

$$H_{\text{sd}} = \frac{J_{\text{sd}}}{V} \sum_{\mathbf{k}\mathbf{k}'\sigma\sigma'} \sum_{I nn'} \mathbf{S}_{nn'} \cdot \mathbf{s}_{\sigma\sigma'} c_{\sigma\mathbf{k}}^\dagger c_{\sigma'\mathbf{k}'} e^{i(\mathbf{k}'-\mathbf{k})\mathbf{R}_I} \hat{P}_{nn'}^I, \quad (2c)$$

$$H_{\text{imp}} = \frac{J_0}{V} \sum_{\mathbf{k}\mathbf{k}'\sigma} \sum_J c_{\sigma\mathbf{k}}^\dagger c_{\sigma\mathbf{k}'} e^{i(\mathbf{k}'-\mathbf{k})\mathbf{R}_J}, \quad (2d)$$

$$H_Z^e = \sum_{\mathbf{k}\sigma\sigma'} \hbar g_e \mu_B \mathbf{B} \cdot \mathbf{s}_{\sigma\sigma'} c_{\sigma\mathbf{k}}^\dagger c_{\sigma'\mathbf{k}}, \quad (2e)$$

$$H_Z^{\text{Mn}} = \sum_{I nn'} \hbar g_{\text{Mn}} \mu_B \mathbf{B} \cdot \mathbf{S}_{nn'} \hat{P}_{nn'}^I, \quad (2f)$$

where  $H_0$  is the single-electron Hamiltonian due to the crystal potential and  $H_Z^e$  and  $H_Z^{\text{Mn}}$  are the carrier and impurity Zeeman energies.

In Eq. (2),  $c_{\sigma\mathbf{k}}^\dagger$  and  $c_{\sigma\mathbf{k}}$  denote the creation and annihilation operators for conduction band electrons with wave vector  $\mathbf{k}$  in the spin subband  $\sigma = \{\uparrow, \downarrow\}$ . The magnetic Mn impurities are described by the operator  $\hat{P}_{nn'}^I = |I, n\rangle\langle I, n'|$  where  $|I, n\rangle$  is the  $n$ th spin state ( $n \in \{-\frac{5}{2}, -\frac{3}{2}, \dots, \frac{5}{2}\}$ ) of the  $I$ th magnetic impurity located at  $\mathbf{R}_I$ . The band structure of the semiconductor is described by  $\hbar\omega_{\mathbf{k}}$ , which we assume to be parabolic  $\omega_{\mathbf{k}} = \frac{\hbar\mathbf{k}^2}{2m^*}$  with effective mass  $m^*$ .  $V$  denotes the volume of the sample.  $\mathbf{S}_{n_1 n_2}$  and  $\mathbf{s}_{\sigma_1 \sigma_2}$  are the vectors with components consisting of spin- $\frac{5}{2}$  and spin- $\frac{1}{2}$  spin matrices for the impurities and the conduction band electrons, respectively, where the unit  $\hbar$  has been substituted into the definition of  $J_{\text{sd}}$  so that  $\mathbf{s}_{\sigma_1 \sigma_2} = \frac{1}{2} \boldsymbol{\sigma}_{\sigma_1 \sigma_2}$ , where  $\boldsymbol{\sigma}_{\sigma_1 \sigma_2}$  are the Pauli matrices. Finally,  $g_e$  and  $g_{\text{Mn}}$  are the  $g$  factors of the electrons and the impurities, respectively, and  $\mu_B$  is the Bohr magneton.

Furthermore, we consider a narrow quantum well where only the lowest confinement state is excited. Projecting the total Hamiltonian in Eq. (2) onto the corresponding subspace is essentially equivalent to replacing the three-dimensional

bulk wave vectors  $\mathbf{k}$  and  $\mathbf{k}'$  by two-dimensional in-plane wave vectors [62].

### B. Quantum kinetic equations of motion

The goal of this article is to study the spin dynamics in DMS after resonant optical excitation with circularly polarized light. To this end, we derive equations of motion for the carrier and impurity density matrices as well as carrier-impurity correlations based on a correlation expansion scheme [56]. The principles of such a theory go back to the cumulant expansion of higher order correlations by Kubo [63]. For investigations of the ultrafast dynamics in semiconductors, correlation expansion methods have been proven very fruitful in the past, in particular, when many-body effects arise due to Coulomb or carrier-phonon interactions [64–66]. A density matrix formalism for the investigation of spin dynamics in semiconductors has been provided by the kinetic spin Bloch equation [48]. The latter, however, were formulated only for uncorrelated single-particle density matrices using the Markov approximation to integrate out correlations arising from the many-body interactions.

In Ref. [56], a density matrix theory was developed for the single-particle density matrices as well as the carrier-impurity correlations built up by the Kondo-like magnetic interaction  $H_{sd}$  in DMS. This theory has been modified in order to describe the spin dynamics in the presence of a finite impurity magnetization [67] and external magnetic fields as well as  $\mathbf{k}$ -dependent effective spin-orbit fields [62]. Here, we extend the quantum kinetic theory further to also include the nonmagnetic impurity interaction  $H_{imp}$ .

Following Ref. [56], we seek to obtain a closed set of equations for the reduced carrier and impurity density matrices as well as for the carrier-impurity correlations:

$$M_{n_1}^{n_2} = \langle \hat{P}_{n_1 n_2}^I \rangle, \quad (3a)$$

$$C_{\sigma_1 \mathbf{k}_1}^{\sigma_2} = \langle c_{\sigma_1 \mathbf{k}_1}^\dagger c_{\sigma_2 \mathbf{k}_1} \rangle, \quad (3b)$$

$$\bar{C}_{\sigma_1 \mathbf{k}_1}^{\sigma_2 \mathbf{k}_2} = V \langle c_{\sigma_1 \mathbf{k}_1}^\dagger c_{\sigma_2 \mathbf{k}_2} e^{i(\mathbf{k}_2 - \mathbf{k}_1) \mathbf{R}_I} \rangle, \quad \text{for } \mathbf{k}_2 \neq \mathbf{k}_1, \quad (3c)$$

$$Q_{\sigma_1 n_1 \mathbf{k}_1}^{\sigma_2 n_2 \mathbf{k}_2} = V \langle c_{\sigma_1 \mathbf{k}_1}^\dagger c_{\sigma_2 \mathbf{k}_2} e^{i(\mathbf{k}_2 - \mathbf{k}_1) \mathbf{R}_I} \hat{P}_{n_1 n_2}^I \rangle, \quad \text{for } \mathbf{k}_2 \neq \mathbf{k}_1. \quad (3d)$$

$M_{n_1}^{n_2}$  and  $C_{\sigma_1 \mathbf{k}_1}^{\sigma_2}$  are the impurity and electron density matrices and  $\bar{C}_{\sigma_1 \mathbf{k}_1}^{\sigma_2 \mathbf{k}_2}$  as well as  $Q_{\sigma_1 n_1 \mathbf{k}_1}^{\sigma_2 n_2 \mathbf{k}_2}$  are the nonmagnetic and magnetic carrier-impurity correlations, respectively. In Eq. (3), the

brackets denote not only the quantum mechanical average of the operators, but also an average over a random distribution of impurity positions, which we assume to be on average homogeneous so that  $\langle e^{i(\mathbf{k}_2 - \mathbf{k}_1) \mathbf{R}_I} \rangle = \delta_{\mathbf{k}_1 \mathbf{k}_2}$ .

The equations of motion for the variables defined in Eq. (3) can be derived using the Heisenberg equations of motion for the corresponding operators. Note, however, that this procedure leads to an infinite hierarchy of variables and equations of motion, since, e.g., the equation of motion for  $\langle c_{\sigma_1 \mathbf{k}_1}^\dagger c_{\sigma_2 \mathbf{k}_2} e^{i(\mathbf{k}_2 - \mathbf{k}_1) \mathbf{R}_I} \hat{P}_{n_1 n_2}^I \rangle$  contains also terms of the form  $\langle c_{\sigma_1 \mathbf{k}_1}^\dagger c_{\sigma \mathbf{k}} e^{i(\mathbf{k} - \mathbf{k}_1) \mathbf{R}_I} e^{i(\mathbf{k}_2 - \mathbf{k}) \mathbf{R}_{I'}} \hat{P}_{n_1 n_2}^I \hat{P}_{n n'}^{I'} \rangle$  for  $I' \neq I$  which cannot be expressed in terms of the variables in Eq. (3). Thus, in order to obtain a closed set of equations, one has to employ a truncation scheme. Here, we follow the procedure of Ref. [56]: we factorize the averages over products of operators and define the true correlations to be the remainder when all combinations of factorizations have been subtracted from the averages. For example, we define (for  $\mathbf{k}_2 \neq \mathbf{k}_1$ )

$$\begin{aligned} \delta \langle c_{\sigma_1 \mathbf{k}_1}^\dagger c_{\sigma_2 \mathbf{k}_2} e^{i(\mathbf{k}_2 - \mathbf{k}_1) \mathbf{R}_I} \hat{P}_{n_1 n_2}^I \rangle \\ := \langle c_{\sigma_1 \mathbf{k}_1}^\dagger c_{\sigma_2 \mathbf{k}_2} e^{i(\mathbf{k}_2 - \mathbf{k}_1) \mathbf{R}_I} \hat{P}_{n_1 n_2}^I \rangle \\ - \left( \langle c_{\sigma_1 \mathbf{k}_1}^\dagger c_{\sigma_2 \mathbf{k}_2} \rangle \langle e^{i(\mathbf{k}_2 - \mathbf{k}_1) \mathbf{R}_I} \rangle \langle \hat{P}_{n_1 n_2}^I \rangle \right) \\ + \langle c_{\sigma_1 \mathbf{k}_1}^\dagger c_{\sigma_2 \mathbf{k}_2} e^{i(\mathbf{k}_2 - \mathbf{k}_1) \mathbf{R}_I} \rangle \langle \hat{P}_{n_1 n_2}^I \rangle \\ + \langle e^{i(\mathbf{k}_2 - \mathbf{k}_1) \mathbf{R}_I} \rangle \langle c_{\sigma_1 \mathbf{k}_1}^\dagger c_{\sigma_2 \mathbf{k}_2} \hat{P}_{n_1 n_2}^I \rangle, \end{aligned} \quad (4)$$

where  $\delta(\dots)$  denotes the true correlations. The basic assumption of the truncation scheme of Ref. [56] is that all correlations higher than  $\delta \langle c_{\sigma_1 \mathbf{k}_1}^\dagger c_{\sigma_2 \mathbf{k}_2} e^{i(\mathbf{k}_2 - \mathbf{k}_1) \mathbf{R}_I} \rangle$  and  $\delta \langle c_{\sigma_1 \mathbf{k}_1}^\dagger c_{\sigma_2 \mathbf{k}_2} e^{i(\mathbf{k}_2 - \mathbf{k}_1) \mathbf{R}_I} \hat{P}_{n_1 n_2}^I \rangle$  are negligible. This assumption results in a closed set of equations of motion for the reduced density matrices and the true correlations. However, it turns out [68] that the equations of motion can be written down in a more condensed form when switching back to the full (nonfactorized) higher-order density matrices as variables, after the higher (true) correlations are neglected. For details of this procedure, the reader is referred to Refs. [56,68].

Applying this truncation scheme to the total Hamiltonian (2) including magnetic and nonmagnetic carrier-impurity interactions as well as the Zeeman terms for carriers and impurities leads to the equations of motion for the variables defined in Eq. (3):

$$-i\hbar \frac{\partial}{\partial t} M_{n_1}^{n_2} = \sum_n \hbar \omega_{Mn} \cdot (\mathbf{S}_{nn_1} M_{n_1}^{n_2} - \mathbf{S}_{n_2 n} M_{n_1}^{n_2}) + \frac{J_{sd}}{V^2} \sum_n \sum_{\mathbf{k}\mathbf{k}'\sigma\sigma'} [\mathbf{S}_{nn_1} \cdot \mathbf{s}_{\sigma\sigma'} Q_{\sigma n \mathbf{k}}^{\sigma' n_2 \mathbf{k}'} - \mathbf{S}_{n_2 n} \cdot \mathbf{s}_{\sigma\sigma'} Q_{\sigma n_1 \mathbf{k}}^{\sigma' n \mathbf{k}'}], \quad (5a)$$

$$\begin{aligned} -i\hbar \frac{\partial}{\partial t} C_{\sigma_1 \mathbf{k}_1}^{\sigma_2} &= \sum_\sigma \hbar \omega_\sigma \cdot (\mathbf{s}_{\sigma\sigma_1} C_{\sigma \mathbf{k}_1}^{\sigma_2} - \mathbf{s}_{\sigma_2 \sigma} C_{\sigma_1 \mathbf{k}_1}^{\sigma_2}) + J_{sd} \frac{N_{Mn}}{V^2} \sum_{nn'} \sum_{\mathbf{k}\sigma} (\mathbf{S}_{nn'} \cdot \mathbf{s}_{\sigma\sigma_1} Q_{\sigma n \mathbf{k}}^{\sigma_2 n' \mathbf{k}_1} - \mathbf{S}_{nn'} \cdot \mathbf{s}_{\sigma_2 \sigma} Q_{\sigma_1 n \mathbf{k}_1}^{\sigma_2 n' \mathbf{k}}) \\ &+ J_0 \frac{N_{imp}}{V^2} \sum_{\mathbf{k}} (\bar{C}_{\sigma_1 \mathbf{k}}^{\sigma_2 \mathbf{k}_1} - \bar{C}_{\sigma_1 \mathbf{k}_1}^{\sigma_2 \mathbf{k}}), \end{aligned} \quad (5b)$$

$$-i\hbar \frac{\partial}{\partial t} Q_{\sigma_1 n_1 \mathbf{k}_1}^{\sigma_2 n_2 \mathbf{k}_2} = \hbar(\omega_{\mathbf{k}_1} - \omega_{\mathbf{k}_2}) Q_{\sigma_1 n_1 \mathbf{k}_1}^{\sigma_2 n_2 \mathbf{k}_2} + b_{\sigma_1 n_1 \mathbf{k}_1}^{\sigma_2 n_2 \mathbf{k}_2 I} + b_{\sigma_1 n_1 \mathbf{k}_1}^{\sigma_2 n_2 \mathbf{k}_2 II} + b_{\sigma_1 n_1 \mathbf{k}_1}^{\sigma_2 n_2 \mathbf{k}_2 III} + b_{\sigma_1 n_1 \mathbf{k}_1}^{\sigma_2 n_2 \mathbf{k}_2 imp}, \quad (5c)$$

$$-i\hbar \frac{\partial}{\partial t} \bar{C}_{\sigma_1 \mathbf{k}_1}^{\sigma_2 \mathbf{k}_2} = \hbar(\omega_{\mathbf{k}_1} - \omega_{\mathbf{k}_2}) \bar{C}_{\sigma_1 \mathbf{k}_1}^{\sigma_2 \mathbf{k}_2} + c_{\sigma_1 \mathbf{k}_1}^{\sigma_2 \mathbf{k}_2 I} + c_{\sigma_1 \mathbf{k}_1}^{\sigma_2 \mathbf{k}_2 II} + c_{\sigma_1 \mathbf{k}_1}^{\sigma_2 \mathbf{k}_2 III} + c_{\sigma_1 \mathbf{k}_1}^{\sigma_2 \mathbf{k}_2 sd} \quad (5d)$$

with

$$b_{\sigma_1 n_1 \mathbf{k}_1}^{\sigma_2 n_2 \mathbf{k}_2 I} = \sum_{n \sigma \sigma'} J_{sd} [\mathbf{S}_{nn_1} \cdot \mathbf{s}_{\sigma \sigma'} (\delta_{\sigma_1 \sigma'} - C_{\sigma_1 \mathbf{k}_1}^{\sigma'}) C_{\sigma \mathbf{k}_2}^{\sigma_2} M_n^{n_2} - \mathbf{S}_{n_2 n} \cdot \mathbf{s}_{\sigma \sigma'} (\delta_{\sigma_2 \sigma} - C_{\sigma \mathbf{k}_2}^{\sigma_2}) C_{\sigma_1 \mathbf{k}_1}^{\sigma'} M_{n_1}^n], \quad (5e)$$

$$b_{\sigma_1 n_1 \mathbf{k}_1}^{\sigma_2 n_2 \mathbf{k}_2 II} = \sum_{\sigma} \hbar \omega_e \cdot (\mathbf{s}_{\sigma \sigma_1} Q_{\sigma n_1 \mathbf{k}_1}^{\sigma_2 n_2 \mathbf{k}_2} - \mathbf{s}_{\sigma_2 \sigma} Q_{\sigma_1 n_1 \mathbf{k}_1}^{\sigma_2 n_2 \mathbf{k}_2}) + \sum_n \hbar \omega_{Mn} \cdot (\mathbf{S}_{nn_1} Q_{\sigma_1 n \mathbf{k}_1}^{\sigma_2 n_2 \mathbf{k}_2} - \mathbf{S}_{n_2 n} Q_{\sigma_1 n_1 \mathbf{k}_1}^{\sigma_2 n_2 \mathbf{k}_2}), \quad (5f)$$

$$b_{\sigma_1 n_1 \mathbf{k}_1}^{\sigma_2 n_2 \mathbf{k}_2 III} = \frac{J_{sd}}{V} \sum_n \sum_{\mathbf{k} \sigma} \left\{ (\mathbf{S}_{nn_1} \cdot \mathbf{s}_{\sigma \sigma_1} Q_{\sigma n \mathbf{k}}^{\sigma_2 n_2 \mathbf{k}_2} - \mathbf{S}_{n_2 n} \cdot \mathbf{s}_{\sigma_2 \sigma} Q_{\sigma_1 n_1 \mathbf{k}_1}^{\sigma_2 n_2 \mathbf{k}_2}) - \sum_{\sigma'} \mathbf{s}_{\sigma \sigma'} \cdot [C_{\sigma_1 \mathbf{k}_1}^{\sigma'} (\mathbf{S}_{nn_1} Q_{\sigma n \mathbf{k}}^{\sigma_2 n_2 \mathbf{k}_2} - \mathbf{S}_{n_2 n} Q_{\sigma_1 n_1 \mathbf{k}_1}^{\sigma_2 n_2 \mathbf{k}_2}) + C_{\sigma \mathbf{k}_2}^{\sigma_2} (\mathbf{S}_{nn_1} Q_{\sigma_1 n \mathbf{k}_1}^{\sigma' n_2 \mathbf{k}} - \mathbf{S}_{n_2 n} Q_{\sigma_1 n_1 \mathbf{k}_1}^{\sigma' n_2 \mathbf{k}})] \right\}, \quad (5g)$$

$$b_{\sigma_1 n_1 \mathbf{k}_1}^{\sigma_2 n_2 \mathbf{k}_2 \text{imp}} = J_0 \left[ (C_{\sigma_1 \mathbf{k}_2}^{\sigma_2} - C_{\sigma_1 \mathbf{k}_1}^{\sigma_2}) M_{n_1}^{n_2} + \frac{1}{V} \sum_{\mathbf{k}} (Q_{\sigma_1 n_1 \mathbf{k}}^{\sigma_2 n_2 \mathbf{k}_2} - Q_{\sigma_1 n_1 \mathbf{k}_1}^{\sigma_2 n_2 \mathbf{k}}) \right], \quad (5h)$$

and

$$c_{\sigma_1 \mathbf{k}_1}^{\sigma_2 \mathbf{k}_2 I} = J_0 (C_{\sigma_1 \mathbf{k}_2}^{\sigma_2} - C_{\sigma_1 \mathbf{k}_1}^{\sigma_2}), \quad (5i)$$

$$c_{\sigma_1 \mathbf{k}_1}^{\sigma_2 \mathbf{k}_2 II} = \sum_{\sigma} \hbar \omega_e \cdot (\mathbf{s}_{\sigma \sigma_1} \bar{C}_{\sigma \mathbf{k}_1}^{\sigma_2 \mathbf{k}_2} - \mathbf{s}_{\sigma_2 \sigma} \bar{C}_{\sigma_1 \mathbf{k}_1}^{\sigma_2 \mathbf{k}_2}), \quad (5j)$$

$$c_{\sigma_1 \mathbf{k}_1}^{\sigma_2 \mathbf{k}_2 III} = \frac{J_0}{V} \sum_{\mathbf{k}} (\bar{C}_{\sigma_1 \mathbf{k}}^{\sigma_2 \mathbf{k}_2} - \bar{C}_{\sigma_1 \mathbf{k}_1}^{\sigma_2 \mathbf{k}_2}), \quad (5k)$$

$$c_{\sigma_1 \mathbf{k}_1}^{\sigma_2 \mathbf{k}_2 \text{sd}} = J_{sd} \sum_{nn'} \sum_{\sigma} M_n^{n'} \mathbf{S}_{nn'} \cdot (\mathbf{s}_{\sigma \sigma_1} C_{\sigma \mathbf{k}_2}^{\sigma_2} - \mathbf{s}_{\sigma_2 \sigma} C_{\sigma_1 \mathbf{k}_1}^{\sigma_2}) + \frac{J_{sd}}{V} \frac{N_{Mn}}{N_{\text{imp}}} \sum_{nn'} \sum_{\mathbf{k} \sigma} \mathbf{S}_{nn'} \cdot (\mathbf{s}_{\sigma \sigma_1} Q_{\sigma n \mathbf{k}}^{\sigma_2 n' \mathbf{k}_2} - \mathbf{s}_{\sigma_2 \sigma} Q_{\sigma_1 n_1 \mathbf{k}_1}^{\sigma_2 n' \mathbf{k}}), \quad (5l)$$

where  $b_{\sigma_1 n_1 \mathbf{k}_1}^{\sigma_2 n_2 \mathbf{k}_2 X}$  are the source terms for the magnetic carrier-impurity correlations,  $c_{\sigma_1 \mathbf{k}_1}^{\sigma_2 \mathbf{k}_2 X}$  are the sources for the nonmagnetic correlations and

$$\omega_{Mn} = g_{Mn} \mu_B \mathbf{B} + \frac{J_{sd}}{\hbar} \frac{1}{V} \sum_{\mathbf{k} \sigma \sigma'} \mathbf{s}_{\sigma \sigma'} C_{\sigma \mathbf{k}}^{\sigma'}, \quad (6a)$$

$$\omega_e = g_e \mu_B \mathbf{B} + \frac{J_{sd}}{\hbar} \frac{N_{Mn}}{V} \sum_{nn'} \mathbf{S}_{nn'} M_n^{n'} \quad (6b)$$

are the mean-field precession frequencies of the impurity and carrier spins, respectively. The first terms on the right-hand side of Eqs. (5a) and (5b) represent the precession of the impurity and carrier spins in the mean field due to the carrier and impurity magnetization as well as the external magnetic field. The second terms in Eqs. (5a) and (5b) describe the effects of the magnetic carrier-impurity correlations on the impurity and carrier density matrices and the last term of Eq. (5b) describes the scattering of carriers at nonmagnetic impurities.

In analogy to the situation without nonmagnetic impurity scattering ( $J_0 = 0$ ) studied in Ref. [68], we label the source terms of the correlations on the right-hand side of the Eqs. (5c) and (5d) as follows. The terms  $b_{\sigma_1 n_1 \mathbf{k}_1}^{\sigma_2 n_2 \mathbf{k}_2 I}$  are the inhomogeneous driving terms depending only on single-particle quantities.  $b_{\sigma_1 n_1 \mathbf{k}_1}^{\sigma_2 n_2 \mathbf{k}_2 II}$  are homogeneous terms which describe a precession-type motion of the correlations in the effective fields  $\omega_e$  and  $\omega_{Mn}$ . The source terms  $b_{\sigma_1 n_1 \mathbf{k}_1}^{\sigma_2 n_2 \mathbf{k}_2 III}$  comprise the driving of the magnetic correlations by other magnetic correlations with different wave vectors and describe a change of the wave

vectors of the correlations due to the  $s$ - $d$  interaction.  $b_{\sigma_1 n_1 \mathbf{k}_1}^{\sigma_2 n_2 \mathbf{k}_2 \text{imp}}$  denotes the contributions to the equation for the magnetic correlations due to the nonmagnetic impurity scattering. The source terms  $c_{\sigma_1 \mathbf{k}_1}^{\sigma_2 \mathbf{k}_2 X}$  for the nonmagnetic correlations are classified analogously. A straightforward but lengthy calculation confirms that Eq. (5) conserve the particle number as well as the total energy comprised of the single-particle contributions and the correlation energies.

### C. Markov limit

Although Eq. (5) can readily be used to calculate the spin dynamics given a set of appropriate initial conditions, it is instructive to derive the Markov limit of the quantum kinetic equations [62,67,68]. On the one hand, this enables us to distinguish the Markovian behavior from genuine quantum kinetic effects. On the other hand, it allows us to derive analytic expressions for the correlation energies and the renormalization of the precession frequencies in the presence of an external magnetic field [59].

The derivation of the Markov limit comprises two steps [62]. First, the equations of motion for the correlations are formally integrated yielding explicit expressions for the correlations in the form of a memory integral. This yields integro-differential equations for the single-particle variables, where the values of the single-particle variables at earlier times enter. Second, the memory integral is eliminated by assuming a  $\delta$ -like short memory.

However, the first step, which involves the formal integration of the carrier-impurity correlations, can, in general, be

complicated. Nevertheless, if the source terms  $b_{\sigma_1 n_1 \mathbf{k}_1}^{\sigma_2 n_2 \mathbf{k}_2 III}$  and  $c_{\sigma_1 \mathbf{k}_1}^{\sigma_2 \mathbf{k}_2 III}$  as well as the correlation-dependent part of  $b_{\sigma_1 n_1 \mathbf{k}_1}^{\sigma_2 n_2 \mathbf{k}_2 imp}$  and  $c_{\sigma_1 \mathbf{k}_1}^{\sigma_2 \mathbf{k}_2 sd}$  are neglected, the formal solution of Eqs. (5c) and (5d) becomes much easier. In absence of nonmagnetic impurity scattering, it has been shown that these source terms are indeed numerically insignificant [68]. Furthermore, a straightforward calculation shows that neglecting these terms also yields a consistent theory with respect to the conservation of the total energy. Whether neglecting the terms  $b_{\sigma_1 n_1 \mathbf{k}_1}^{\sigma_2 n_2 \mathbf{k}_2 III}$ ,  $c_{\sigma_1 \mathbf{k}_1}^{\sigma_2 \mathbf{k}_2 III}$  and the correlation-dependent parts of  $b_{\sigma_1 n_1 \mathbf{k}_1}^{\sigma_2 n_2 \mathbf{k}_2 imp}$  and  $c_{\sigma_1 \mathbf{k}_1}^{\sigma_2 \mathbf{k}_2 sd}$  is indeed a good approximation in the presence of nonmagnetic impurity scattering can be tested by comparing the numerical results of the quantum kinetic equations with and without accounting for these source terms.

Neglecting the aforementioned source terms in Eq. (5), we first formulate a set of quantum kinetic equations for the new dynamical variables:

$$\langle S^i \rangle = \sum_{n_1 n_2} S_{n_1 n_2}^i M_{n_1}^{n_2}, \quad (7a)$$

$$n_{\mathbf{k}} = \sum_{\sigma} C_{\sigma \mathbf{k}}^{\sigma}, \quad (7b)$$

$$s_{\mathbf{k}}^i = \sum_{\sigma_1 \sigma_2} s_{\sigma_1 \sigma_2}^i C_{\sigma_1 \mathbf{k}}^{\sigma_2}, \quad (7c)$$

$$\bar{C}_{\mathbf{k}_1}^{\alpha \mathbf{k}_2} = \sum_{\sigma_1 \sigma_2} s_{\sigma_1 \sigma_2}^{\alpha} \bar{C}_{\sigma_1 \mathbf{k}_1}^{\sigma_2 \mathbf{k}_2}, \quad (7d)$$

$$Q_{l \mathbf{k}_1}^{\alpha \mathbf{k}_2} = \sum_{\sigma_1 \sigma_2} \sum_{n_1 n_2} s_{\sigma_1 \sigma_2}^{\alpha} S_{n_1 n_2}^l Q_{\sigma_1 n_1 \mathbf{k}_1}^{\sigma_2 n_2 \mathbf{k}_2}, \quad (7e)$$

where  $\langle S \rangle$  is the average impurity spin and  $n_{\mathbf{k}}$  and  $s_{\mathbf{k}}$  are the occupation density and spin density of the carrier states with wave vector  $\mathbf{k}$ , respectively.  $\bar{C}_{\mathbf{k}_1}^{\alpha \mathbf{k}_2}$  as well as  $Q_{l \mathbf{k}_1}^{\alpha \mathbf{k}_2}$  comprise the nonmagnetic and magnetic carrier-impurity correlations. In Eq. (7), we use a notation in which the Latin indices are in the range  $\{1, 2, 3\}$ , while the Greek indices also include the value 0, where  $s_{\sigma_1 \sigma_2}^0 = \delta_{\sigma_1 \sigma_2}$  is the  $2 \times 2$  identity matrix. The corresponding equations of motion for the variables defined in Eq. (7) are explicitly given in the Appendix.

Note that the source terms  $b_{l \mathbf{k}_1}^{\alpha \mathbf{k}_2 I}$  for the correlations  $Q_{l \mathbf{k}_1}^{\alpha \mathbf{k}_2}$  depend on the second moments of the impurity spins  $\langle S^i S^j \rangle = \sum_{n_1 n_2 n_3} S_{n_1 n_2}^i S_{n_2 n_3}^j M_{n_1}^{n_3}$  for which we do not present equations of motions, although such equations can, in principle, be derived from Eq. (5). Here, we use the fact that for typical sample parameters the optically induced carrier density is usually much lower than the impurity concentration, so that the average impurity spin only changes marginally over time [68]. For the numerical calculations, we assume that the impurity density matrix can be approximately described as being in thermal equilibrium at all times where the effective impurity spin temperature  $T_{Mn}$  can be obtained from the value of  $\langle S \rangle$ . From this thermally occupied density matrix, the second moments  $\langle S^i S^j \rangle$  consistent with  $\langle S \rangle$  can be calculated in each time step.

The equations of motion for the variables defined in Eq. (7) are the starting point for the formal integration of the

correlations. Note that Eqs. (A1d)–(A1g) for the correlations  $Q_{l \mathbf{k}_1}^{\alpha \mathbf{k}_2}$  and  $\bar{C}_{\mathbf{k}_1}^{\alpha \mathbf{k}_2}$  can be transformed into the general form

$$\begin{aligned} \frac{\partial}{\partial t} Q_{\mathbf{k}_1}^{\mathbf{k}_2} &= -i(\omega_{\mathbf{k}_2} - \omega_{\mathbf{k}_1}) Q_{\mathbf{k}_1}^{\mathbf{k}_2} + i\chi_1 \omega_e Q_{\mathbf{k}_1}^{\mathbf{k}_2} \\ &+ i\chi_2 \omega_{Mn} Q_{\mathbf{k}_1}^{\mathbf{k}_2} + b_{\mathbf{k}_1}^{\mathbf{k}_2 I}, \end{aligned} \quad (8)$$

where  $\chi_1, \chi_2 \in \{-1, 0, 1\}$  and the terms proportional to  $\omega_e = |\omega_e|$  and  $\omega_{Mn} = |\omega_{Mn}|$  originate from the precession of the correlations described by the source terms  $b_{\sigma_1 n_1 \mathbf{k}_1}^{\sigma_2 n_2 \mathbf{k}_2 II}$  and  $c_{\sigma_1 \mathbf{k}_1}^{\sigma_2 \mathbf{k}_2 II}$ .

The term  $b_{\mathbf{k}_1}^{\mathbf{k}_2 I}$  here denotes the contributions from the source terms  $b_{\sigma_1 n_1 \mathbf{k}_1}^{\sigma_2 n_2 \mathbf{k}_2 I}$ ,  $c_{\sigma_1 \mathbf{k}_1}^{\sigma_2 \mathbf{k}_2 I}$ ,  $b_{\sigma_1 n_1 \mathbf{k}_1}^{\sigma_2 n_2 \mathbf{k}_2 imp}$  and  $c_{\sigma_1 \mathbf{k}_1}^{\sigma_2 \mathbf{k}_2 sd}$  and only depends on the single-particle variables. The formal integration of Eq. (8) yields

$$Q_{\mathbf{k}_1}^{\mathbf{k}_2}(t) = \int_0^t dt' e^{i[\omega_{\mathbf{k}_2} - (\omega_{\mathbf{k}_1} + \chi_1 \omega_e + \chi_2 \omega_{Mn})](t-t')} b_{\mathbf{k}_1}^{\mathbf{k}_2 I}(t'). \quad (9)$$

The Markov limit consists of assuming a short memory, i.e., the assumption that the correlations at time  $t$  depend only significantly on the single-particle variables at the same time  $t$ , so that one is inclined to evaluate  $b_{\mathbf{k}_1}^{\mathbf{k}_2 I}(t')$  in Eq. (9) at  $t' = t$  and to draw the source term out of the integral. However, first, one has to make sure that the source terms are indeed slowly changing variables. For example, the carrier spin can precess rapidly about an external magnetic field. Therefore we first analyze the mean-field precession of the single-particle quantities and split the source terms into parts oscillating with some frequencies  $\omega$  of the form

$$b_{\mathbf{k}_1}^{\mathbf{k}_2 I}(t') \stackrel{MF}{=} \sum_{\omega} \sum_{\chi \in \{-1, 0, 1\}} e^{i\chi\omega(t'-t)} b_{\mathbf{k}_1}^{\mathbf{k}_2 \omega, \chi}(t'). \quad (10)$$

Then, the different oscillating parts  $b_{\mathbf{k}_1}^{\mathbf{k}_2 \omega, \chi}(t)$  can be drawn out of the memory integral and the remaining integral can be solved in the limit of large times  $t$  [62]:

$$\int_0^t dt' e^{i\Delta\omega(t'-t)} \xrightarrow{t \rightarrow \infty} \pi \delta(\Delta\omega) - \frac{i}{\Delta\omega}. \quad (11)$$

This procedure yields particularly transparent results in the case where the external magnetic field and the impurity magnetization are collinear, as is usually the case when the number of impurities exceeds the number of quasifree carriers ( $N_{Mn} \gg N_e$ ), and the impurity density matrix is initially occupied thermally. Choosing the direction of  $\omega_e$  as a reference and defining  $s_{\mathbf{k}_1}^{\parallel} := \mathbf{s} \cdot \frac{\omega_e}{\omega_e}$ ,  $S^{\parallel} := \hat{S} \cdot \frac{\omega_e}{\omega_e}$  and  $\omega_{Mn}^{\parallel} := \omega_{Mn} \cdot \frac{\omega_e}{\omega_e}$ , the Markovian equations obtained for the spin-up and spin-down occupations and the perpendicular carrier spin component with respect to the direction of  $\omega_e$ ,

$$n_{\mathbf{k}_1}^{\uparrow/\downarrow} := \frac{n_{\mathbf{k}_1}}{2} \pm s_{\mathbf{k}_1}^{\parallel}, \quad (12a)$$

$$\mathbf{s}_{\mathbf{k}_1}^{\perp} := \mathbf{s}_{\mathbf{k}_1} - \frac{\omega_e}{\omega_e} s_{\mathbf{k}_1}^{\parallel}, \quad (12b)$$

are given by

$$\begin{aligned} \frac{\partial}{\partial t} n_{\mathbf{k}_1}^{\uparrow/\downarrow} = & \frac{\pi}{\hbar^2 V^2} \sum_{\mathbf{k}_2} \left\{ \delta(\omega_{\mathbf{k}_2} - \omega_{\mathbf{k}_1}) \left[ J_{sd}^2 N_{Mn} \frac{1}{2} \langle S^{\perp 2} \rangle \pm J_{sd} J_0 (N_{Mn} + N_{imp}) \langle S^{\parallel} \rangle + 2J_0^2 N_{imp} \right] (n_{\mathbf{k}_2}^{\uparrow/\downarrow} - n_{\mathbf{k}_1}^{\uparrow/\downarrow}) \right. \\ & \left. + \delta[\omega_{\mathbf{k}_2} - (\omega_{\mathbf{k}_1} \pm (\omega_e - \omega_{Mn}^{\parallel}))] J_{sd}^2 N_{Mn} \left[ \left( \langle S^{\perp 2} \rangle \pm \frac{1}{2} \langle S^{\parallel} \rangle \right) (1 - n_{\mathbf{k}_1}^{\uparrow/\downarrow}) n_{\mathbf{k}_2}^{\downarrow/\uparrow} - \left( \langle S^{\perp 2} \rangle \mp \frac{1}{2} \langle S^{\parallel} \rangle \right) (1 - n_{\mathbf{k}_2}^{\downarrow/\uparrow}) n_{\mathbf{k}_1}^{\uparrow/\downarrow} \right] \right\}, \end{aligned} \quad (13a)$$

$$\begin{aligned} \frac{\partial}{\partial t} \mathbf{s}_{\mathbf{k}_1}^{\perp} = & -\frac{\pi}{\hbar^2 V^2} \sum_{\mathbf{k}_2} \left\{ \delta(\omega_{\mathbf{k}_2} - \omega_{\mathbf{k}_1}) \left[ J_{sd}^2 N_{Mn} \frac{1}{2} \langle S^{\perp 2} \rangle (\mathbf{s}_{\mathbf{k}_2}^{\perp} + \mathbf{s}_{\mathbf{k}_1}^{\perp}) - 2J_0^2 N_{imp} (\mathbf{s}_{\mathbf{k}_2}^{\perp} - \mathbf{s}_{\mathbf{k}_1}^{\perp}) \right] \right. \\ & + \delta[\omega_{\mathbf{k}_2} - (\omega_{\mathbf{k}_1} + (\omega_e - \omega_{Mn}^{\parallel}))] \frac{1}{2} \left( \langle S^{\perp 2} \rangle - \frac{1}{2} \langle S^{\parallel} \rangle (1 - 2n_{\mathbf{k}_2}^{\downarrow}) \right) \mathbf{s}_{\mathbf{k}_1}^{\perp} \\ & + \delta[\omega_{\mathbf{k}_2} - (\omega_{\mathbf{k}_1} - (\omega_e - \omega_{Mn}^{\parallel}))] \frac{1}{2} \left( \langle S^{\perp 2} \rangle + \frac{1}{2} \langle S^{\parallel} \rangle (1 - 2n_{\mathbf{k}_2}^{\uparrow}) \right) \mathbf{s}_{\mathbf{k}_1}^{\perp} \left. \right\} \\ & + \omega_e \times \mathbf{s}_{\mathbf{k}_1}^{\perp} + \frac{1}{\hbar^2 V^2} \sum_{\mathbf{k}_2} \left\{ -\frac{J_{sd} J_0}{\omega_{\mathbf{k}_2} - \omega_{\mathbf{k}_1}} \langle \mathbf{S} \rangle \times [(N_{imp} - N_{Mn}) \mathbf{s}_{\mathbf{k}_2}^{\perp} + (N_{Mn} + N_{imp}) \mathbf{s}_{\mathbf{k}_1}^{\perp}] \right. \\ & - \frac{J_{sd}^2 N_{Mn}}{\omega_{\mathbf{k}_2} - (\omega_{\mathbf{k}_1} + (\omega_e - \omega_{Mn}^{\parallel}))} \frac{1}{2} \left( \langle S^{\perp 2} \rangle - \frac{1}{2} \langle S^{\parallel} \rangle (1 - 2n_{\mathbf{k}_2}^{\downarrow}) \right) \left( \frac{\omega_e}{\omega_e} \times \mathbf{s}_{\mathbf{k}_1}^{\perp} \right) \\ & \left. + \frac{J_{sd}^2 N_{Mn}}{\omega_{\mathbf{k}_2} - (\omega_{\mathbf{k}_1} - (\omega_e - \omega_{Mn}^{\parallel}))} \frac{1}{2} \left( \langle S^{\perp 2} \rangle + \frac{1}{2} \langle S^{\parallel} \rangle (1 - 2n_{\mathbf{k}_2}^{\uparrow}) \right) \left( \frac{\omega_e}{\omega_e} \times \mathbf{s}_{\mathbf{k}_1}^{\perp} \right) \right\}. \end{aligned} \quad (13b)$$

The first line on the right-hand side of Eq. (13a), which is proportional to  $n_{\mathbf{k}_2}^{\uparrow/\downarrow} - n_{\mathbf{k}_1}^{\uparrow/\downarrow}$ , describes a redistribution of occupations of spin-up and spin-down states within a shell of defined kinetic energy via the term proportional to  $\delta(\omega_{\mathbf{k}_2} - \omega_{\mathbf{k}_1})$ . For a parabolic band structure, this implies a redistribution between states with the same modulus  $|\mathbf{k}|$  of the wave vector  $\mathbf{k}$ , while the total carrier spin remains unchanged. If accompanied by a wave-vector dependent magnetic field like a Rashba or the Dresselhaus field, this term leads to a D'yakonov-Perel'-type suppression of the spin dephasing. Here, however, we do not consider any wave vector dependent field and the system under investigation is isotropic in  $\mathbf{k}$  space, so that the first line in Eq. (13a) has no influence on the dynamics of the total spin. The second line in Eq. (13a) describes a spin-flip scattering from the spin-up band to the spin-down band and vice versa. Since these bands are energetically split by  $\hbar\omega_e$  and a flip of a carrier spin involves a corresponding flip of an impurity spin in the opposite direction, which requires a magnetic (Zeeman) energy of  $\hbar\omega_{Mn}^{\parallel}$ , the total magnetic energy released in a spin-flip process is  $\pm\hbar(\omega_e - \omega_{Mn}^{\parallel})$ . Thus  $\delta[\omega_{\mathbf{k}_2} - (\omega_{\mathbf{k}_1} \pm (\omega_e - \omega_{Mn}^{\parallel}))]$  ensures a conservation of the total single-particle energies in the Markov limit. It is noteworthy that, if the mean-field dynamics of the source terms as in Eq. (10) is not correctly taken into account, other energetic shifts are obtained in the  $\delta$  function, which yields equations in the Markov limit that are not consistent with the conservation of the single-particle energies [62]. Note also that the right-hand side of Eq. (13a) correctly deals with Pauli blocking effects. Because the nonmagnetic impurity scattering enters in the equations of motion (13a) for the spin-up and spin-down occupation only via the first line which plays no role in an isotropic system, it has no influence on the spin dynamics in the Markov limit.

The first three lines in Eq. (13b) for the perpendicular carrier spin component, which are proportional to  $\delta$  functions, indicate an exponential decay of the perpendicular carrier spin component towards zero. The last three lines describe a precession of the perpendicular carrier spin component. The mean-field precession frequency  $\omega_e$  is renormalized by the carrier-impurity correlations. This renormalization originates from the imaginary part of the memory integral in Eq. (11). Besides the terms proportional to  $\frac{1}{\omega_{\mathbf{k}_2} - (\omega_{\mathbf{k}_1} \pm (\omega_e - \omega_{Mn}^{\parallel}))}$ , which are also present when only the magnetic  $s$ - $d$  interaction is taken into account [59], the nonmagnetic impurity scattering introduces another contribution which is a cross-term, i.e., it is absent when either the magnetic or the nonmagnetic impurity scattering is absent, which can be seen from the fact that it is proportional to the product of  $J_{sd}$  and  $J_0$ . In the quasicontinuous limit, the sum over  $\mathbf{k}_2$  can be replaced by an integral over the spectral density of states. In quasi-two-dimensional systems like quantum wells, the spectral density of states  $D(\omega) = \frac{Am^*}{2\pi\hbar}$  is constant. Thus the frequency renormalization can be integrated and yields logarithmic divergences

$$\begin{aligned} \sum_{\mathbf{k}_2} \frac{1}{\omega_{\mathbf{k}_2} - \omega_0} &= \int_0^{\omega_{BZ}} d\omega D(\omega) \frac{1}{\omega - \omega_0} \\ &= \frac{Am^*}{2\pi\hbar} \ln \left| \frac{\omega_{BZ} - \omega_0}{\omega_0} \right| \end{aligned} \quad (14)$$

at the poles  $\omega_0 = \omega_{\mathbf{k}_1}$  and  $\omega_0 = \omega_{\mathbf{k}_1} \pm (\omega_e - \omega_{Mn}^{\parallel})$ . These logarithmic divergences are similar to the ones obtained in the discussion of the Kondo effect in metals with magnetic impurities [40]. Despite the formal divergence, the summation over a nonsingular carrier distribution always leads to a finite

value of the precession frequency of the total carrier spin, since the logarithm is integrable [62]. From Eq. (14), one can see that the cut-off energy  $\hbar\omega_{\text{BZ}}$ , which corresponds to the width of the conduction band and is typically of the order of 1 eV, enters as a new model parameter in the theory and cannot be eliminated by assuming that  $\omega_{\text{BZ}} \rightarrow \infty$ , since then the frequency renormalization also diverges. As a consequence, the Markovian expression for the frequency renormalization can only give an order-of-magnitude estimation and a more detailed treatment of the band structure is necessary if a quantitatively more accurate description is required.

For the special case of zero external magnetic field, vanishing impurity magnetization and low carrier densities, equation (13) are equivalent to the simple rate equations

$$\frac{\partial}{\partial t} \mathbf{s}_{\mathbf{k}_1} = -\frac{1}{\tau} \mathbf{s}_{\mathbf{k}_1}, \quad (15)$$

where the rates coincide with that obtained by Fermi's golden rule or equivalent approaches [19,22,30,31,47–52]. In two dimensions, one obtains [58]

$$\frac{1}{\tau^{2D}} = \frac{35}{12} \frac{J_{\text{sd}}^2 m^* N_{\text{Mn}}}{\hbar^3 V d}. \quad (16)$$

#### D. Correlation energy

In Eqs. (9) to (11), Markovian expressions for the carrier-impurity correlations are derived as functionals of the carrier and impurity variables. Using these expressions, it is straightforward to also obtain analytic expressions for the carrier-impurity correlation energies as functionals of the carrier spins and occupations [62]. Splitting the averages over the magnetic and nonmagnetic carrier-impurity interactions into mean-field and correlated contributions,

$$\langle H_{\text{sd}} \rangle = \langle H_{\text{sd}}^{\text{MF}} \rangle + \langle H_{\text{sd}}^{\text{cor}} \rangle, \quad (17a)$$

$$\langle H_{\text{imp}} \rangle = \langle H_{\text{imp}}^{\text{MF}} \rangle + \langle H_{\text{imp}}^{\text{cor}} \rangle, \quad (17b)$$

$$\langle H_{\text{sd}}^{\text{MF}} \rangle = \frac{J_{\text{sd}} N_{\text{Mn}}}{V} \sum_{\mathbf{k}} \langle \mathbf{S} \rangle \cdot \mathbf{s}_{\mathbf{k}}, \quad (17c)$$

$$\langle H_{\text{sd}}^{\text{cor}} \rangle = \frac{J_{\text{sd}} N_{\text{Mn}}}{V^2} \sum_{\mathbf{k}, \mathbf{k}'} \sum_i Q_{i\mathbf{k}}^{i\mathbf{k}'}, \quad (17d)$$

$$\langle H_{\text{imp}}^{\text{MF}} \rangle = \frac{J_0 N_{\text{imp}}}{V} \sum_{\mathbf{k}} n_{\mathbf{k}}, \quad (17e)$$

$$\langle H_{\text{imp}}^{\text{cor}} \rangle = \frac{J_0 N_{\text{imp}}}{V^2} \sum_{\mathbf{k}, \mathbf{k}'} \bar{C}_{\mathbf{k}}^{0\mathbf{k}'}, \quad (17f)$$

one obtains in the Markov limit

$$\begin{aligned} \langle H_{\text{sd}}^{\text{cor}} \rangle = & -\frac{J_{\text{sd}} N_{\text{Mn}}}{V^2} \sum_{\mathbf{k}_1 \mathbf{k}_2} \left\{ \frac{\frac{1}{2} J_{\text{sd}} \langle S^{\parallel 2} \rangle n_{\mathbf{k}_1} + 2J_0 \langle S^{\parallel} \rangle s_{\mathbf{k}_1}^{\parallel}}{\omega_{\mathbf{k}_2} - \omega_{\mathbf{k}_1}} \right. \\ & + \frac{J_{\text{sd}} (\langle S^{\perp 2} \rangle - \frac{1}{2} \langle S^{\parallel} \rangle) (1 - n_{\mathbf{k}_2}^{\downarrow}) n_{\mathbf{k}_1}^{\uparrow}}{\omega_{\mathbf{k}_2} - (\omega_{\mathbf{k}_1} + (\omega_{\text{e}} - \omega_{\text{Mn}}^{\parallel}))} \\ & \left. + \frac{J_{\text{sd}} (\langle S^{\perp 2} \rangle + \frac{1}{2} \langle S^{\parallel} \rangle) (1 - n_{\mathbf{k}_2}^{\uparrow}) n_{\mathbf{k}_1}^{\downarrow}}{\omega_{\mathbf{k}_2} - (\omega_{\mathbf{k}_1} - (\omega_{\text{e}} - \omega_{\text{Mn}}^{\parallel}))} \right\}, \quad (18a) \end{aligned}$$

$$\langle H_{\text{imp}}^{\text{cor}} \rangle = -2 \frac{J_0 N_{\text{imp}}}{V^2} \sum_{\mathbf{k}_1 \mathbf{k}_2} \frac{J_0 n_{\mathbf{k}_1} + J_{\text{sd}} \langle S^{\parallel} \rangle s_{\mathbf{k}_1}^{\parallel}}{\omega_{\mathbf{k}_2} - \omega_{\mathbf{k}_1}}. \quad (18b)$$

Equation (18) have the same poles as Eq. (13b) for the frequency renormalization and, thus, also contain formally logarithmic divergences in two-dimensional systems.

### III. RESULTS

After having derived the quantum kinetic equations for the description of the spin dynamics in DMS including magnetic and nonmagnetic scattering and having obtained rate-type Markovian equations, we now present results of numerical simulations. Here, we focus on the case of a 4-nm-wide  $\text{Cd}_{0.93}\text{Mn}_{0.07}\text{Te}$  quantum well. For this material, the magnetic coupling constant is  $J_{\text{sd}} = -15 \text{ meV nm}^3$  ( $N_0 J_{\text{sd}} = -220 \text{ meV}$ ) [45], while the nonmagnetic coupling constant is approximately  $J_0 = 110 \text{ meV nm}^3$  ( $N_0 J_0 = 1.6 \text{ eV}$ ) [44], where  $N_0$  is the number of unit cells per unit volume. Furthermore, we use a conduction band effective mass of  $m^* = 0.1 m_0$  and assume that the impurity magnetization is described by a thermal distribution at a temperature of  $T = 2 \text{ K}$  and the  $g$  factors of the conduction band carriers and Mn impurities are  $g_{\text{e}} = -1.77$  and  $g_{\text{Mn}} = 2$ , respectively [60]. We assume that there are no other scattering centers present beside the Mn impurities, which implies  $N_{\text{imp}} = N_{\text{Mn}}$ .

Here, we are interested in pump-pulse measurements, where the spin dynamics of the carrier system is probed after resonant excitation with a circularly polarized light beam that directly induces a spin polarization of the optically excited carriers via spin selection rules. We assume that the spins of the optically excited holes are pinned due to the strong heavy-hole–light-hole splitting in narrow quantum wells and only the dynamics of the conduction band electron spin is of interest. For our calculations, we further assume that an ultrafast circularly polarized Gaussian pump pulse resonant to the band gap has excited spin-up electrons into the conduction band at time  $t = 0$  and we use a corresponding Gaussian spectral electron occupation of the spin-up conduction band as an initial value for the carrier density matrix. This assumption requires that the pump pulse is weak enough, so that Pauli blocking and saturation effects during the excitation, e.g., Rabi flops, are negligible. Here, we consider a pump pulse with full width at half maximum (FWHM) pulse duration of about 350 fs, which translates into a spectral width of the initial Gaussian occupation of spin-up electrons with standard deviation of  $E_s = 0.4 \text{ meV}$ . Earlier studies where only the magnetic carrier-impurity interaction was taken into account showed that the predictions of such initial value calculations are very well reproduced if the optical excitation is directly taken into account via the corresponding light-matter interaction Hamiltonian in dipole approximation [69].

With these initial values, the equations of motion are integrated numerically using a Runge-Kutta algorithm. To this end, the  $\mathbf{k}$  space is discretized and truncated, i.e., only taken into account up to a cutoff energy of  $\hbar\omega_{\text{BZ}} = 40 \text{ meV}$ . Moreover, we assume that the initial occupation of the carrier density matrix is isotropic in the two-dimensional  $\mathbf{k}$  space. Then, the values of the density matrices and the correlations

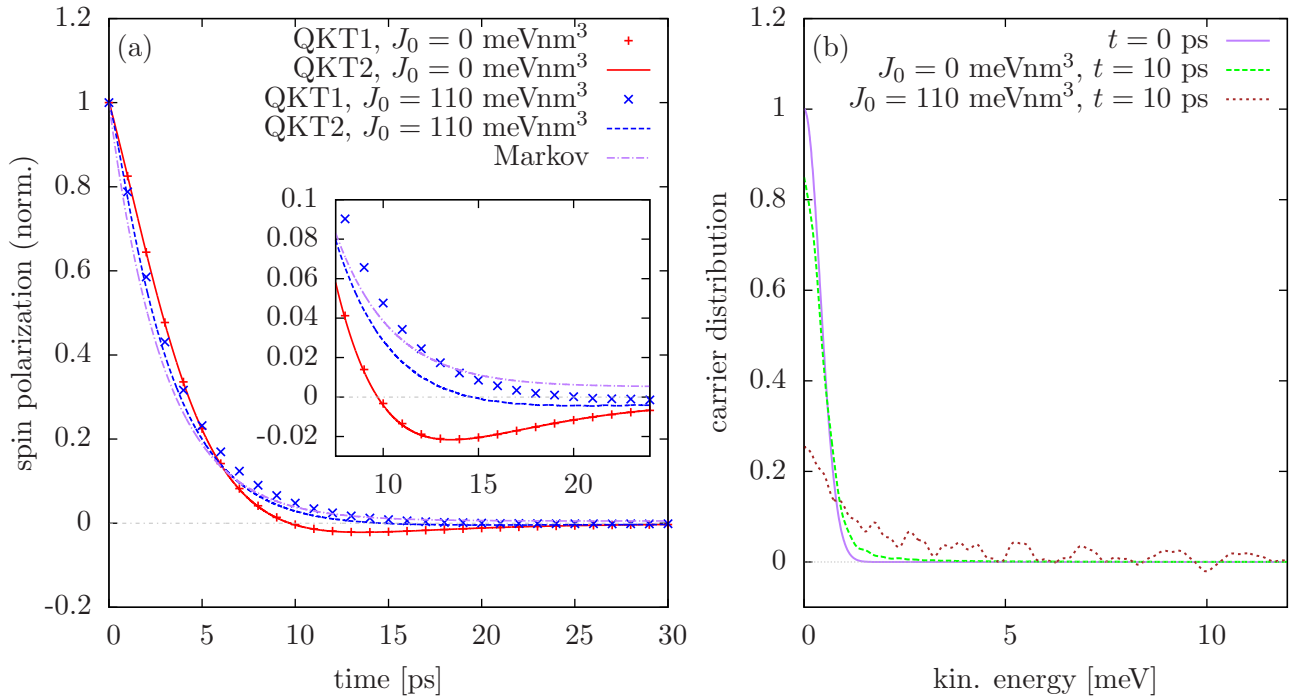


FIG. 1. (a) Time evolution of the carrier spin for zero magnetic field with ( $J = 110 \text{ meV nm}^3$ ) and without ( $J = 0$ ) nonmagnetic impurity scattering. QKT1 (points) denotes the results according to the full quantum kinetic equation (5), while QKT2 (lines) describes the results of the reduced set of equation (A1). The purple dash-dotted line shows the results of the Markovian equation (13), which is independent of nonmagnetic impurity scattering. The inset shows a magnification of the region where the quantum kinetic theory for  $J_0 = 0$  predicts a nonmonotonic behavior. (b) Occupation of carrier states at  $t = 0$  and  $t = 10$  ps for the calculations with and without nonmagnetic impurity scattering.

depend for all times only on the modulus  $|\mathbf{k}|$  of the wave vector  $\mathbf{k}$  and not its polar angle in the two-dimensional  $\mathbf{k}$  space. This implies that for each  $\mathbf{k}$  index of a density matrix or correlation, only a one-dimensional continuum has to be discretized, which speeds up the numerics significantly.

We first discuss the spin dynamics in the conduction band of a  $\text{Cd}_{0.93}\text{Mn}_{0.07}\text{Te}$  quantum well for zero magnetic field with a focus on the impact of nonmagnetic impurity scattering on the spin dynamics and investigate the redistribution of carriers in  $\mathbf{k}$  space as well as the build-up of correlation energy. Then, we study the spin dynamics in the valence band in a simplified model. Finally, we investigate the spin dynamics in the presence of an external magnetic field parallel and perpendicular to the carrier spin polarization and discuss, in the latter case, how the nonmagnetic impurity scattering affects the carrier spin precession frequencies.

### A. Zero magnetic field

Figure 1(a) shows the time evolution of an initially polarized electron spin in a  $\text{Cd}_{0.93}\text{Mn}_{0.07}\text{Te}$  quantum well for vanishing magnetic field. The Markovian equation (13), which are not affected by nonmagnetic impurity scattering for the case considered here and are therefore independent of  $J_0$ , predict a simple exponential decay of the carrier spin, which is transferred to the impurities. Note that due to  $N_{\text{Mn}} \gg N_e$ , the asymptotic value of the carrier spin for long times  $t$  is close to zero, since the impurities act as a spin bath. If only the magnetic spin-flip scattering is accounted for ( $J_0 = 0$ ), the time

evolution according to the quantum kinetic theory is nonmonotonic and shows an overshoot below the asymptotic value. Such an overshoot has already been discussed in Refs. [57,58]. Here, we find that these non-Markovian effects are strongly suppressed in the calculations including nonmagnetic impurity scattering ( $J_0 = 110 \text{ meV nm}^3$ ) and the time evolution of the total spin follows the Markovian dynamics more closely. An exponential fit to the dynamics of the full quantum kinetic theory yields an effective spin transfer rate about 15% smaller than the Markovian rate in Eq. (16). Interestingly, while the full quantum kinetic equation (5) yield identical results as the reduced set of equation (A1) in the case without nonmagnetic impurity scattering, deviations between both approaches can be clearly seen when the nonmagnetic impurity scattering is taken into account.

In order to understand the suppression of the nonmonotonic features in the spin dynamics with nonmagnetic impurity scattering, it is useful to recapitulate the findings of Ref. [57], where the origin of the non-Markovian behavior of the spin dynamics in absence of nonmagnetic impurity scattering was discussed: it was found that the depth of the memory induced by the correlations is of the order of the inverse energetic distance of the carrier state under consideration to the band edge times  $\hbar$ . Memory effects become insignificant if the kinetic energy of the carrier  $\hbar\omega_{\mathbf{k}_1}$  is much higher than the energy scale of the carrier-impurity spin transfer rate  $\frac{\hbar}{\tau}$ . For the parameters used in the simulations, one obtains from Eq. (16) a value of  $\tau^{2D} = 2.97$  ps and therefore  $\frac{\hbar}{\tau} \approx 0.22$  meV. Figure 1(b) shows the redistribution of carriers

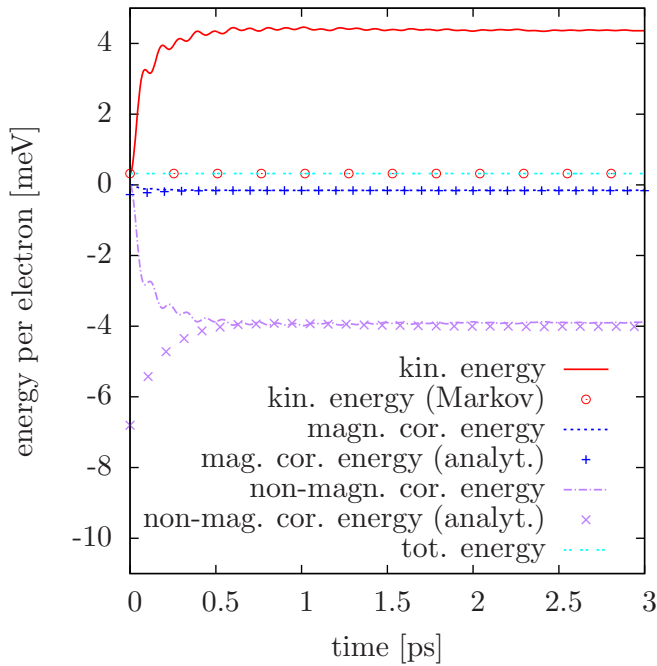


FIG. 2. Kinetic energy (red line), magnetic correlation energy (blue line), non-magnetic correlation energy (purple line) and total energy (cyan line) per electron for the quantum kinetic calculation shown in Fig. 1 with  $J_0 = 110 \text{ meVnm}^3$ . The red circles show the kinetic energy obtained from the Markovian calculation in Fig. 1. The pluses and crosses depict the results according to the analytic Markovian expressions for the correlation energies in Eq. (18) evaluated using the carrier distribution of the quantum kinetic calculation at selected time steps.

in the calculations with and without nonmagnetic impurity scattering. One can clearly see that, while without nonmagnetic impurity scattering the carrier distribution at  $t = 10 \text{ ps}$  is only slightly broadened, including the nonmagnetic impurity scatterings leads to a drastic redistribution of carriers to states many meV away from the initial distribution. For these states, the memory is very short compared with the spin relaxation time and therefore the Markovian approximation is justified.

The redistribution of carriers to states several meV away from the band edge raises questions about the conservation of energy, since for zero magnetic field the mean-field energy of the system is comprised of only the kinetic energy of the carriers. In the quantum kinetic calculations, however, we also consider the carrier-impurity correlations which introduce correlation energies that are not captured in a simple single-particle picture. The different contributions to the total energy over the course of time for the simulations presented in Fig. 1 are shown in Fig. 2. There, it is shown that the average kinetic energy per electron increases from the initial value of the order of the width of the initial carrier distribution to a much larger value of about 4 meV on a time scale of about 0.5 ps. This energy is mostly provided by a decrease of nonmagnetic correlation energy from zero to a negative value. The magnetic correlation energy is comparatively small since the magnetic coupling constant  $J_{sd}$  is about one order of magnitude smaller than the nonmagnetic coupling constant  $J_0$ . The pluses and crosses in Fig. 2 show the results of the analytic expressions

(18) for the correlation energies evaluated using the carrier distributions of the full quantum kinetic theory in the respective time steps. The analytic results are found to coincide with the values extracted from the quantum kinetic theory after the first 0.5 ps. Even though the analytic expressions for the correlation energies are obtained within the Markovian description, it should be noted that in the Markovian equations of motion (13) for the spins and occupations only single-particle energies are considered for evaluating the energy balance. As in our case, the single particle energies comprise only the kinetic energies of the carriers, the latter are constant in the Markovian description in sharp contrast to the quantum kinetic treatment. Note also that the total energy comprised of single-particle and correlation energies remains constant in the quantum kinetic simulations, which provides a further test for the numerics.

### B. Valence band

The fact that in the conduction band of a  $\text{Cd}_{1-x}\text{Mn}_x\text{Te}$  quantum well the nonmagnetic scattering at the impurities suppresses the characteristic nonmonotonic features of genuine quantum kinetic behavior raises the question whether this statement is true in general and non-Markovian effects always only change the spin dynamics quantitatively. In this section, we provide an example of a situation where the non-Markovian features are not suppressed due to impurity scattering.

We consider now the valence band of a  $\text{Cd}_{1-x}\text{Mn}_x\text{Te}$  quantum well. The details of the valence band structure in a quantum well are influenced by, e.g., spin-orbit coupling, strain or the shape of the confinement potential. In principle, these effects can be described in terms of  $\mathbf{k}\cdot\mathbf{p}$  theory as contributions to a Kane or Luttinger Hamiltonian [70], which can be mapped onto  $\hbar\omega_{\mathbf{k}_1}$  and  $\hbar\omega_e \cdot \mathbf{s}_{\sigma_1\sigma_2}$  in the quantum kinetic equation (5) provided  $\omega_e$  is considered  $\mathbf{k}$ -dependent and  $\mathbf{s}_{\sigma_1\sigma_2}$  is generalized to a basis of traceless Hermitian  $4 \times 4$  matrices for the description of the heavy- and light-hole subbands. However, the matrix elements of the Luttinger Hamiltonian depend explicitly on the polar angle of the wave vector  $\mathbf{k}$  in  $\mathbf{k}$  space that has to be resolved in numerical calculations, which increases the numerical demands enormously. Thus a realistic description of the band structure is beyond the scope of this article. Instead, we perform a model study, where we assume that heavy-hole and light-hole bands are degenerate. In this case, we can use the quantum kinetic theory derived for the conduction band and take the material parameters for the heavy holes. The magnetic coupling constant in the valence band is  $J_{pd} = 60 \text{ meV nm}^3$  [45] and the heavy-hole mass is  $m_h = 0.7m_0$  [71]. The difference of the band gaps between CdTe and zinc-blende MnTe of about 1.6 eV is split into the conduction and valence band offsets by a ratio of 14:1 [72]. Thus one obtains a value for the nonmagnetic coupling constant in the valence band of about  $J_0 = 7 \text{ meV nm}^3$ . The results of the quantum kinetic simulations for these parameters are shown in Fig. 3.

In comparison with the conduction band, the four times larger magnetic coupling constant in the valence band leads to much stronger non-Markovian effects. In particular, one finds not a single overshoot, but pronounced oscillations of the spin polarization about its asymptotic value. In Fig. 3, the calculations with and without accounting for nonmagnetic

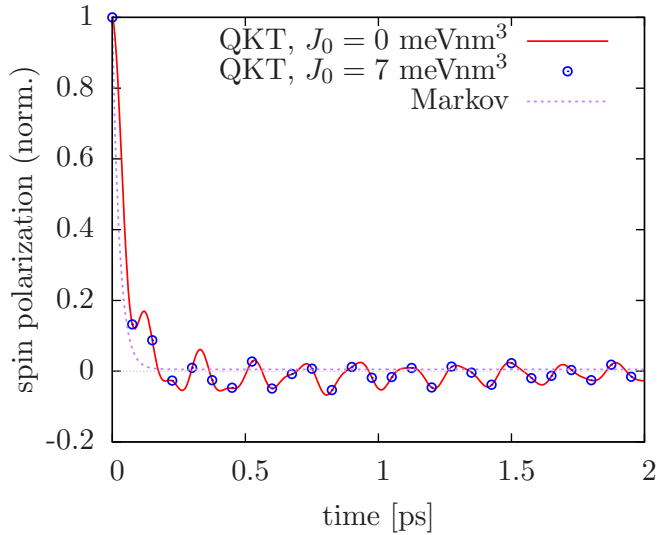


FIG. 3. Spin dynamics in a degenerate valence band of a  $\text{Cd}_{0.93}\text{Mn}_{0.07}\text{Te}$  quantum well with and without accounting for nonmagnetic impurity scattering.

impurity scattering yield virtually identical results. Thus, due to the fact that in the valence band the nonmagnetic coupling constant is much smaller than the magnetic coupling constant, no suppression of non-Markovian effects in the spin dynamics is observed.

### C. Finite magnetic field: Faraday configuration

Next, we investigate the effects of nonmagnetic impurity scattering on the spin dynamics in DMS in the presence of an external magnetic field. In this section, we study the case in which the external field and the initial carrier spins are parallel, which is known as the Faraday configuration. This case has

also been considered in Ref. [60], but without accounting for nonmagnetic impurity scattering.

In Fig. 4(a), the time evolution of the carrier spin polarization parallel to an external magnetic field  $B = 100$  mT is shown. Note that the nonmonotonic behavior that can be seen in the case without an external magnetic field is suppressed for finite external fields even if the nonmagnetic scattering is disregarded. The most striking feature in the time evolution of the carrier spin polarization is that the Markovian result and the quantum kinetic simulations predict very different asymptotic values of the spin polarization at long times  $t$ .

As discussed in Ref. [60], the different stationary values are related to a broadening of the distribution of scattered carriers in the spin-down band, which is shown in Fig. 4(b). Note that the broadening of the carrier distribution is not primarily an effect of energy-time uncertainty, which is commonly found in quantum kinetic studies [73,74], since the width of the distribution does not shrink significantly over the course of time [60]. Rather, it is a consequence of the build-up of correlation energy which enables deviations from the conservation of the single-particle energies in spin-flip scattering processes.

In the Markov limit, the stationary value is obtained when a balance between scattering from the spin-up to the spin-down band and vice versa is reached. In the quantum kinetic calculations, the distribution of the scattered carriers is broadened, so that also spin-down states below the threshold  $\hbar\omega_e - \hbar\omega_{\text{Mn}}^{\parallel}$  are occupied, whose back-scattering is suppressed since there are no states in the spin-up band with the matching single-particle energies. If additionally the nonmagnetic impurity scattering is taken into account, the scattered impurity distribution is even broader and more spin-down states with kinetic energies below  $\hbar\omega_e - \hbar\omega_{\text{Mn}}^{\parallel}$  are occupied, so that the back-scattering is more strongly suppressed and the deviation of the asymptotic value of the spin polarization from the Markovian value is even larger.

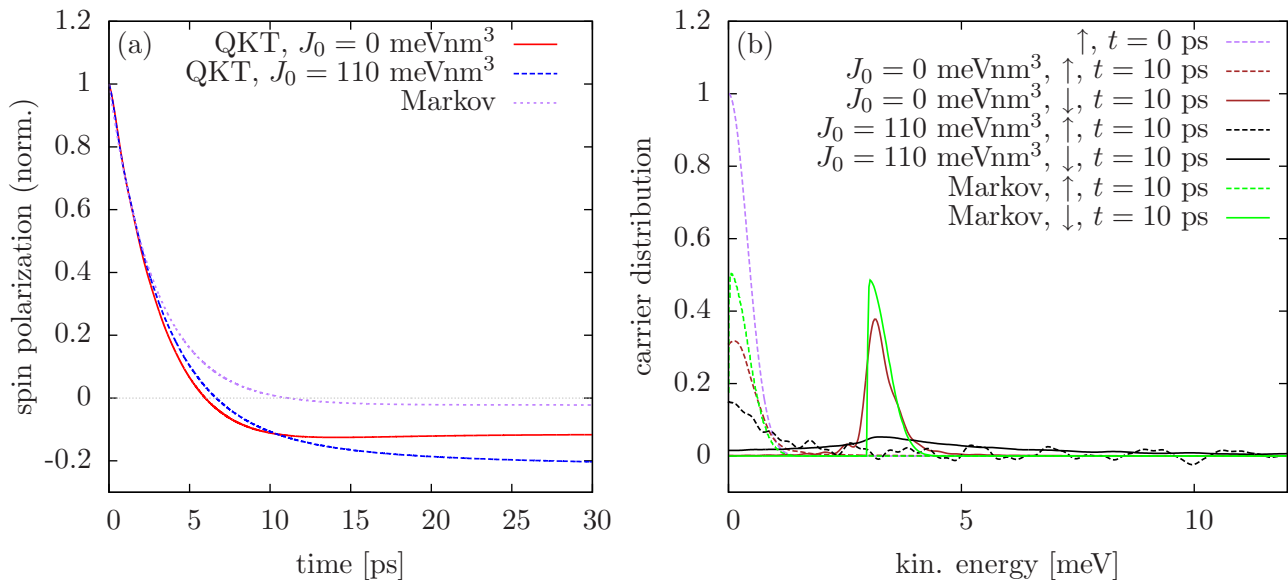


FIG. 4. (a) Time evolution of the carrier spin polarization parallel to an external magnetic field ( $B = 100$  mT). (b) Spin-up ( $\uparrow$ ) and spin-down occupations ( $\downarrow$ ) at  $t = 0$  and 10 ps.

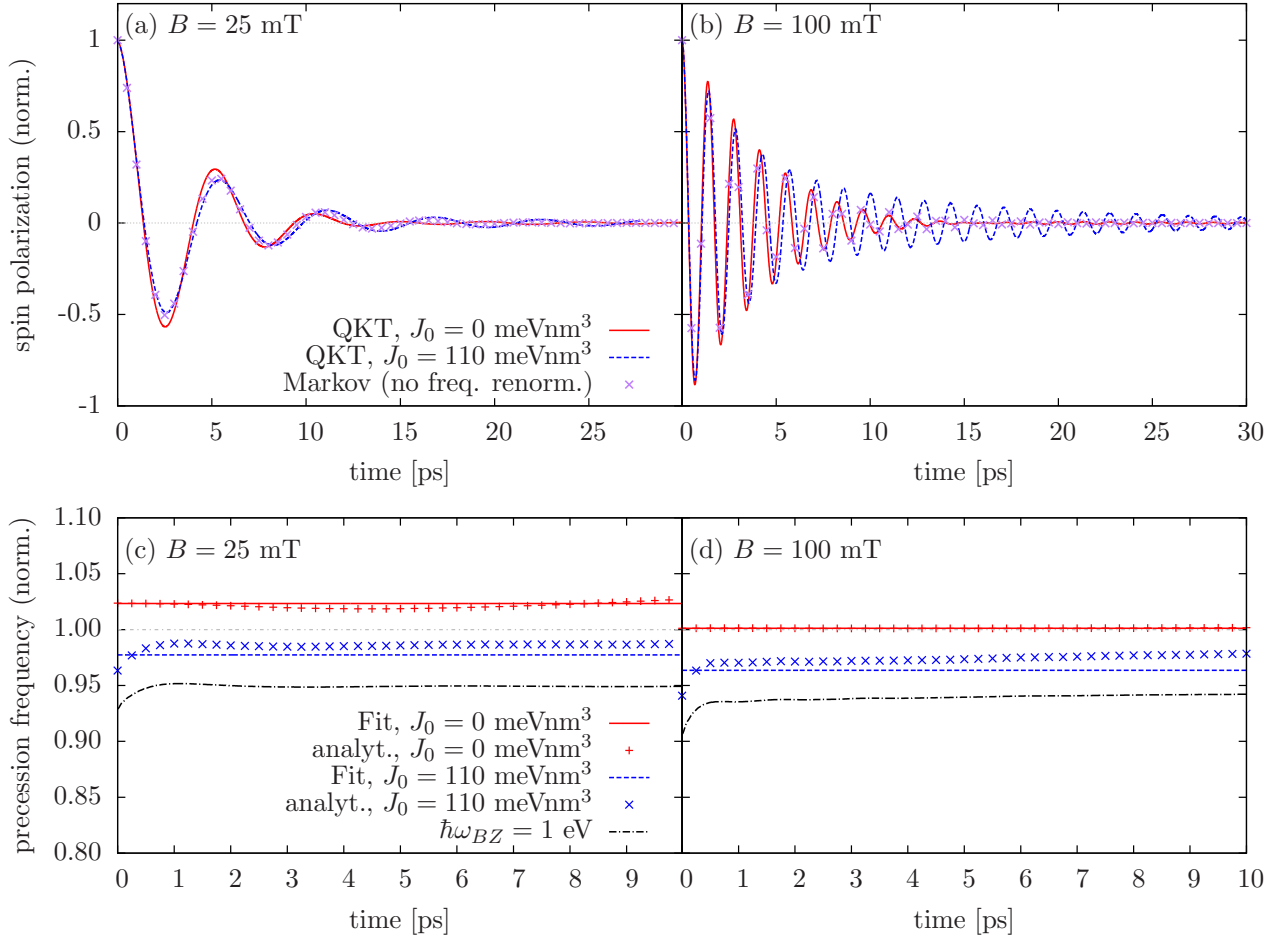


FIG. 5. (a) and (b) Time evolution of the carrier spin polarization for (a)  $B = 25$  and (b)  $100$  mT (b) using the quantum kinetic equation (5) and the Markovian equations Eq. (13b), where the terms responsible for the frequency renormalization in the Markovian equations have been dropped. The precession frequency normalized with respect to its mean-field value  $\omega_e$  is shown in (c) and (d) using a fit of an exponentially decaying cosine to the quantum kinetic results and the analytic expressions obtained from Eq. (13b) and the occupations from the quantum kinetic calculations. The black dash-dotted lines in (c) and (d) show the analytic results for a cut-off energy of  $\hbar\omega_{BZ} = 1$  eV.

#### D. Finite magnetic field: Voigt configuration

The situation in which an external magnetic field and the optically induced carrier spin polarization are perpendicular to each other is usually referred to as the Voigt configuration and is the subject of this section. In this situation, the carrier spin precesses about the effective magnetic field  $\omega_e$  due to the external field and the impurity magnetization. As shown in Ref. [59], where the nonmagnetic impurity scattering was disregarded, the carrier-impurity correlations are responsible for a renormalization of the precession frequency. There, it was also shown that the strength of this renormalization depends on the details of the carrier distribution and the strength of the effective field  $\omega_e$ .

In Fig. 5(a), we present simulations of the spin dynamics in a DMS in Voigt geometry for an external magnetic field of  $B = 25$  mT, which corresponds to a situation with  $|\langle \mathbf{S} \rangle| \approx 0.05$ , where the magnetic-correlation-induced frequency renormalization according to Ref. [59] is particularly strong. Simulations with ( $J_0 = 110$  meVnm<sup>3</sup>) and without ( $J_0 = 0$ ) accounting for the nonmagnetic impurity scattering are compared to Markovian calculations based on Eq. (13). Note that for the Markovian calculation shown in Fig. 5

the frequency renormalization was not taken into account. The results of all simulations shown in Fig. 5(a) are very similar and follow closely the form of an exponentially damped cosine. Note that at long times, the phases of the oscillations of the calculations accounting for nonmagnetic impurity scattering matches the Markovian calculation without frequency renormalization, while accounting only for magnetic spin-flip scattering leads to oscillations with a slightly higher frequency.

The frequency renormalization for the simulations shown in Fig. 5(a) is presented in Fig. 5(c), where an exponentially decaying cosine is fit to the quantum kinetic results and, for comparison, the total precession frequency including the correlation-induced renormalization in the Markovian description in Eq. (13b) evaluated using the spin-up and spin-down occupations of the quantum kinetic simulations is depicted. Due to the time evolution of the occupations, also the renormalization predicted by Eq. (13b) becomes a function of time, which, however, is for all times close to the constant extracted by fitting the quantum kinetic result. The calculations without nonmagnetic impurity scattering predict an increase of the carrier spin precession frequency of about 2%–3% with respect to the mean-field value  $\omega_e$ , which is consistent with

the findings of Ref. [59]. On the other hand, the contribution from the nonmagnetic carrier-impurity correlations leads to a decrease of the precession frequency which partially cancels the contribution from the magnetic correlations.

In Figs. 5(b) and 5(d), the time evolution of the carrier spin polarization and the frequency renormalization are shown for an external magnetic field of  $B = 100$  mT. In this case, the envelope of the spin polarization decays only exponentially for the calculations without nonmagnetic impurity scattering. For  $J_0 = 110$  meV nm<sup>3</sup>, the spin polarization follows the exponential decay of the simulation with  $J_0 = 0$  only up to about 5 ps. After that, it decays much slower, which is a new non-Markovian effect that is absent if the nonmagnetic impurity scattering is disregarded. As can be seen in Fig. 5(d), the frequency renormalization due to the magnetic interaction alone is almost zero. Nevertheless, when the nonmagnetic carrier-impurity correlations are taken into account, the precession frequency shows a decrease of about 2%–3%. Thus, in contrast to the correlation-induced renormalization in absence of nonmagnetic scattering where the renormalization is only observable for a very narrow set of initial conditions [59], including the nonmagnetic carrier-impurity interaction results in a significant renormalization for a much broader set of excitation conditions.

It is noteworthy that the frequency renormalization in the quantum kinetic calculations is well reproduced by the Markovian expression in Eq. (13b). The numerical demands of the full quantum kinetic equations require a restriction of the conduction band width  $\hbar\omega_{\text{BZ}}$  used in the calculations to a few tens of meV. However, in realistic band structures, the band widths are of the order of eV. In order to give an order-of-magnitude estimation of the frequency renormalization for such band widths, we present in Figs. 5(c) and 5(d) also the results of the Markovian expression for the frequency renormalizations using the value of  $\hbar\omega_{\text{BZ}} = 1$  eV together with the occupations obtained in the quantum kinetic calculations for  $\hbar\omega_{\text{BZ}} = 40$  meV. This estimation yields a renormalization of the precession frequencies due to the combined effects of magnetic and nonmagnetic scattering of about 5%–7%. A quantitatively more accurate description requires a more detailed treatment of the band structure, which is beyond the scope of this article.

Note also that the frequency renormalization due to the nonmagnetic carrier-impurity correlations is dominated by a cross-term proportional to  $J_{\text{sd}}J_0$  [cf. fourth line in Eq. (13b)]. Thus, the sign of the frequency renormalization depends on the relative signs of the coupling constants  $J_{\text{sd}}$  and  $J_0$ . In principle, this allows a determination of the sign of the magnetic coupling

constant  $J_{\text{sd}}$ , which cannot be obtained directly, e.g., by measuring the giant Zeeman splitting of excitons [45].

#### IV. CONCLUSION

We have investigated the influence of nonmagnetic impurity scattering at Mn impurities on the spin dynamics in Cd<sub>1-x</sub>Mn<sub>x</sub>Te diluted magnetic semiconductors. To this end, we have developed a quantum kinetic theory taking the magnetic and nonmagnetic carrier-impurity correlations into account. The Markov limit of the quantum kinetic equations is derived in order to distinguish the Markovian dynamics from genuine quantum kinetic effects.

In the Markov approximation, the nonmagnetic impurity scattering is found to have no influence on the spin dynamics in DMS whatsoever. However, in narrow Cd<sub>1-x</sub>Mn<sub>x</sub>Te quantum wells where the spin dynamics induced by the magnetic carrier-impurity interaction alone is predicted to show significant non-Markovian features, such as overshoots of the carrier spin polarization below its asymptotic value for long times [58], these nonmonotonocities are found to be strongly suppressed when also the nonmagnetic impurity scattering is accounted for. In contrast, in the valence band of Cd<sub>1-x</sub>Mn<sub>x</sub>Te, the nonmagnetic carrier-impurity interaction for holes is much weaker than the magnetic interaction and therefore does not influence the spin dynamics visibly.

Furthermore, many-body correlation effects, such as the renormalization of the carrier spin precession frequency and the build-up of correlation energy, are significantly enhanced by the nonmagnetic carrier-impurity interaction. For example, the correlation energy built up by the nonmagnetic carrier-impurity interaction is more than one order of magnitude larger than the contribution due to the magnetic interaction alone. This is also the reason why significant deviations from the conservation of the single-particle energies during spin-flip scattering events are obtained when nonmagnetic impurity scattering is accounted for on a quantum kinetic level. As a consequence, the carriers are redistributed in  $\mathbf{k}$  space. The most prominent manifestation of this redistribution is the change of the asymptotic value of the carrier spin polarization at long times in the presence of an external magnetic field parallel to the optically induced carrier spin polarization.

#### ACKNOWLEDGMENTS

We gratefully acknowledge the financial support from the Universidad de Buenos Aires, project UBACyT 2014-2017 No. 20020130100514BA and, from CONICET, project PIP 11220110100091.

#### APPENDIX: REDUCED SET OF EQUATIONS OF MOTIONS

The equations of motions for the variables defined in Eq. (7) are

$$\frac{\partial}{\partial t} \langle S^l \rangle = \sum_{im} \epsilon_{lim} \omega_{\text{Mn}}^i \langle S^m \rangle + \frac{J_{\text{sd}}}{V} \sum_{\mathbf{k}\mathbf{k}'} \sum_{im} \epsilon_{lim} \text{Re} \{ Q_{m\mathbf{k}}^{i\mathbf{k}'} \}, \quad (\text{A1a})$$

$$\frac{\partial}{\partial t} n_{\mathbf{k}_1} = \frac{J_{\text{sd}} N_{\text{Mn}}}{\hbar V^2} \sum_{\mathbf{k}} \sum_i 2\text{Im} \{ Q_{i\mathbf{k}_1}^{i\mathbf{k}} \} + \frac{J_0 N_{\text{imp}}}{\hbar V^2} \sum_{\mathbf{k}} 2\text{Im} \{ \bar{C}_{\mathbf{k}_1}^{0\mathbf{k}} \}, \quad (\text{A1b})$$

$$\frac{\partial}{\partial t} s_{k_1}^l = \sum_{ij} \epsilon_{lij} \omega_e^i s_{k_1}^j + \frac{J_{sd} N_{Mn}}{\hbar V^2} \sum_{\mathbf{k}} \left[ \frac{1}{2} \text{Im} \{ Q_{l k_1}^{0k} \} + \sum_{ij} \epsilon_{lij} \text{Re} \{ Q_{i k_1}^{jk} \} \right] + \frac{J_0 N_{\text{imp}}}{\hbar V^2} \sum_{\mathbf{k}} 2 \text{Im} \{ \bar{C}_{k_1}^{lk} \}, \quad (\text{A1c})$$

$$\frac{\partial}{\partial t} Q_{l k_1}^{0k_2} = -i(\omega_{k_2} - \omega_{k_1}) Q_{l k_1}^{0k_2} + \sum_{ii'} \epsilon_{lii'} \omega_{Mn}^i Q_{i' k_1}^{0k_2} + \frac{i}{\hbar} b_{l k_1}^{0k_2 I} + \frac{i}{\hbar} b_{l k_1}^{0k_2 \text{imp}}, \quad (\text{A1d})$$

$$\frac{\partial}{\partial t} Q_{l k_1}^{jk_2} = -i(\omega_{k_2} - \omega_{k_1}) Q_{l k_1}^{jk_2} + \sum_{ii'} \epsilon_{jii'} \omega_e^i Q_{i' k_1}^{jk_2} + \sum_{ii'} \epsilon_{lii'} \omega_{Mn}^i Q_{i' k_1}^{jk_2} + \frac{i}{\hbar} b_{l k_1}^{jk_2 I} + \frac{i}{\hbar} b_{l k_1}^{jk_2 \text{imp}}, \quad (\text{A1e})$$

$$\frac{\partial}{\partial t} \bar{C}_{k_1}^{0k_2} = -i(\omega_{k_2} - \omega_{k_1}) \bar{C}_{k_1}^{0k_2} + \frac{i}{\hbar} c_{k_1}^{0k_2 I} + \frac{i}{\hbar} c_{k_1}^{0k_2 \text{sd}}, \quad (\text{A1f})$$

$$\frac{\partial}{\partial t} \bar{C}_{k_1}^{jk_2} = -i(\omega_{k_2} - \omega_{k_1}) \bar{C}_{k_1}^{jk_2} + \sum_{ii'} \epsilon_{jii'} \omega_e^i \bar{C}_{k_1}^{i' k_2} + \frac{i}{\hbar} c_{k_1}^{jk_2 I} + \frac{i}{\hbar} c_{k_1}^{jk_2 \text{sd}}, \quad (\text{A1g})$$

with

$$b_{l k_1}^{0k_2 I} = J_{sd} \sum_i \left[ \text{Re} \{ \langle S^i S^l \rangle \} (s_{k_2}^i - s_{k_1}^i) + i \sum_m \epsilon_{ilm} \frac{\langle S^m \rangle}{2} ((1 - n_{k_1}) s_{k_2}^i + (1 - n_{k_2}) s_{k_1}^i) + \langle S^i \rangle (s_{k_1}^l s_{k_2}^i - s_{k_1}^i s_{k_2}^l) \right], \quad (\text{A1h})$$

$$b_{l k_1}^{jk_2 I} = J_{sd} \sum_i \left[ \text{Re} \{ \langle S^i S^l \rangle \} \left[ \delta_{ij} \left( \frac{n_{k_2}}{4} - \frac{n_{k_1}}{4} \right) + \frac{i}{2} \epsilon_{ijk} (s_{k_1}^k + s_{k_2}^k) \right] + \frac{i}{2} \sum_m \epsilon_{ilm} \langle S^m \rangle \left[ \delta_{ij} \frac{n_{k_1} + n_{k_2} - n_{k_1} n_{k_2}}{4} \right. \right. \\ \left. \left. + \delta_{ij} \mathbf{s}_{k_1} \cdot \mathbf{s}_{k_2} - (s_{k_1}^i s_{k_2}^j + s_{k_2}^i s_{k_1}^j) + \frac{i}{2} \epsilon_{ijk} ((1 - n_{k_1}) s_{k_2}^k - (1 - n_{k_2}) s_{k_1}^k) \right] \right], \quad (\text{A1i})$$

$$b_{l k_1}^{0k_2 \text{imp}} = J_0 \langle S^l \rangle (n_{k_2} - n_{k_1}), \quad (\text{A1j})$$

$$b_{l k_1}^{jk_2 \text{imp}} = J_0 \langle S^l \rangle (s_{k_2}^j - s_{k_1}^j), \quad (\text{A1k})$$

$$c_{k_1}^{0k_2 I} = J_0 (n_{k_2} - n_{k_1}), \quad (\text{A1l})$$

$$c_{k_1}^{jk_2 I} = J_0 (s_{k_2}^j - s_{k_1}^j), \quad (\text{A1m})$$

$$c_{k_1}^{0k_2 \text{sd}} = J_{sd} \langle S^i \rangle (s_{k_2}^i - s_{k_1}^i), \quad (\text{A1n})$$

$$c_{k_1}^{jk_2 \text{sd}} = J_{sd} \left[ \frac{1}{4} \langle S^j \rangle (n_{k_2} - n_{k_1}) + \frac{i}{2} \epsilon_{ijk} \langle S^i \rangle (s_{k_2}^k + s_{k_1}^k) \right]. \quad (\text{A1o})$$

- 
- [1] M. N. Baibich, J. M. Broto, A. Fert, F. Nguyen Van Dau, F. Petroff, P. Etienne, G. Creuzet, A. Friederich, and J. Chazelas, *Phys. Rev. Lett.* **61**, 2472 (1988).
- [2] S. A. Wolf, D. D. Awschalom, R. A. Buhrman, J. M. Daughton, S. von Molnár, M. L. Roukes, A. Y. Chtchelkanova, and D. M. Treger, *Science* **294**, 1488 (2001).
- [3] S. Datta and B. Das, *Appl. Phys. Lett.* **56**, 665 (1990).
- [4] D. Awschalom and M. Flatté, *Nat. Phys.* **3**, 153 (2007).
- [5] I. Žutić, J. Fabian, and S. Das Sarma, *Rev. Mod. Phys.* **76**, 323 (2004).
- [6] T. Dietl, *Nat. Mater.* **9**, 965 (2010).
- [7] H. Ohno, *Nat. Mater.* **9**, 952 (2010).
- [8] T. Dietl and H. Ohno, *Rev. Mod. Phys.* **86**, 187 (2014).
- [9] T. Dietl, H. Ohno, F. Matsukura, J. Cibert, and D. Ferrand, *Science* **287**, 1019 (2000).
- [10] Z. Ben Cheikh, S. Cronenberger, M. Vladimirova, D. Scalbert, F. Perez, and T. Wojtowicz, *Phys. Rev. B* **88**, 201306 (2013).
- [11] Y. S. Chen, M. Wiater, G. Karczewski, T. Wojtowicz, and G. Bacher, *Phys. Rev. B* **87**, 155301 (2013).
- [12] S. Cronenberger, M. Vladimirova, S. V. Andreev, M. B. Lifshits, and D. Scalbert, *Phys. Rev. Lett.* **110**, 077403 (2013).
- [13] J. Debus, V. Y. Ivanov, S. M. Ryabchenko, D. R. Yakovlev, A. A. Maksimov, Y. G. Semenov, D. Braukmann, J. Rautert, U. Löw, M. Godlewski, A. Waag, and M. Bayer, *Phys. Rev. B* **93**, 195307 (2016).
- [14] J. Debus, A. A. Maksimov, D. Dunker, D. R. Yakovlev, E. V. Filatov, I. I. Tartakovskii, V. Y. Ivanov, A. Waag, and M. Bayer, *Phys. Status Solidi B* **251**, 1694 (2014).
- [15] A. A. Maksimov, D. R. Yakovlev, J. Debus, I. I. Tartakovskii, A. Waag, G. Karczewski, T. Wojtowicz, J. Kossut, and M. Bayer, *Phys. Rev. B* **82**, 035211 (2010).
- [16] F. Perez, J. Cibert, M. Vladimirova, and D. Scalbert, *Phys. Rev. B* **83**, 075311 (2011).
- [17] M. D. Kapetanakis, I. E. Perakis, K. J. Wickey, C. Piermarocchi, and J. Wang, *Phys. Rev. Lett.* **103**, 047404 (2009).
- [18] M. D. Kapetanakis and I. E. Perakis, *Phys. Rev. Lett.* **101**, 097201 (2008).
- [19] H. Krenn, K. Kaltenecker, T. Dietl, J. Spałek, and G. Bauer, *Phys. Rev. B* **39**, 10918 (1989).

- [20] S. A. Crooker, D. D. Awschalom, J. J. Baumberg, F. Flack, and N. Samarth, *Phys. Rev. B* **56**, 7574 (1997).
- [21] P. Barate, S. Cronenberger, M. Vladimirova, D. Scalbert, F. Perez, J. Gómez, B. Jusserand, H. Boukari, D. Ferrand, H. Mariette, J. Cibert, and M. Nawrocki, *Phys. Rev. B* **82**, 075306 (2010).
- [22] J. H. Jiang, Y. Zhou, T. Korn, C. Schüller, and M. W. Wu, *Phys. Rev. B* **79**, 155201 (2009).
- [23] H. Ohno, A. Shen, F. Matsukura, A. Oiwa, A. Endo, S. Katsumoto, and Y. Iye, *Appl. Phys. Lett.* **69**, 363 (1996).
- [24] R. Fiederling, M. Keim, G. Reuscher, W. Ossau, G. Schmidt, A. Waag, and L. W. Molenkamp, *Nature (London)* **402**, 787 (1999).
- [25] J. K. Furdyna, *J. Appl. Phys.* **64**, R29 (1988).
- [26] T. Jungwirth, J. Sinova, J. Mašek, J. Kučera, and A. H. MacDonald, *Rev. Mod. Phys.* **78**, 809 (2006).
- [27] G. Tang and W. Nolting, *Phys. Rev. B* **75**, 024426 (2007).
- [28] M. D. Kapetanakis, J. Wang, and I. E. Perakis, *J. Opt. Soc. Am. B* **29**, A95 (2012).
- [29] O. Morandi, P.-A. Hervieux, and G. Manfredi, *New J. Phys.* **11**, 073010 (2009).
- [30] O. Morandi, P.-A. Hervieux, and G. Manfredi, *Phys. Rev. B* **81**, 155309 (2010).
- [31] A. Baral and H. C. Schneider, *Phys. Rev. B* **91**, 100402 (2015).
- [32] P. A. Wolff and J. Warnock, *J. Appl. Phys.* **55**, 2300 (1984).
- [33] J. Spałek, *Phys. Rev. B* **30**, 5345 (1984).
- [34] P. A. Wolff, R. N. Bhatt, and A. C. Durst, *J. Appl. Phys.* **79**, 5196 (1996).
- [35] D. E. Angelescu and R. N. Bhatt, *Phys. Rev. B* **65**, 075211 (2002).
- [36] J. König, H.-H. Lin, and A. H. MacDonald, *Phys. Rev. Lett.* **84**, 5628 (2000).
- [37] F. J. Teran, M. Potemski, D. K. Maude, D. Plantier, A. K. Hassan, A. Sachrajda, Z. Wilamowski, J. Jaroszynski, T. Wojtowicz, and G. Karczewski, *Phys. Rev. Lett.* **91**, 077201 (2003).
- [38] R. Akimoto, K. Ando, F. Sasaki, S. Kobayashi, and T. Tani, *Phys. Rev. B* **56**, 9726 (1997).
- [39] C. Camilleri, F. Teppe, D. Scalbert, Y. G. Semenov, M. Nawrocki, M. Dyakonov, J. Cibert, S. Tatarenko, and T. Wojtowicz, *Phys. Rev. B* **64**, 085331 (2001).
- [40] J. Kondo, *Prog. Theor. Phys.* **32**, 37 (1964).
- [41] J. Kossut, *Phys. Status Solidi B* **72**, 359 (1975).
- [42] B. E. Larson, K. C. Hass, H. Ehrenreich, and A. E. Carlsson, *Phys. Rev. B* **37**, 4137 (1988).
- [43] J. R. Schrieffer and P. A. Wolff, *Phys. Rev.* **149**, 491 (1966).
- [44] A. Twardowski, M. Nawrocki, and J. Ginter, *Phys. Status Solidi B* **96**, 497 (1979).
- [45] Edited by J. Kossut and J. Gaj, *Introduction to the Physics of Diluted Magnetic Semiconductors*, Springer Series in Materials Science Vol. 144 (Springer, Berlin, 2011).
- [46] N. Gonzalez Szewacki, E. Przedziecka, E. Dynowska, P. Boguslawski, and J. Kossut, *Acta Phys. Pol. A* **106**, 233 (2004).
- [47] G. Bastard and L. L. Chang, *Phys. Rev. B* **41**, 7899 (1990).
- [48] M. W. Wu, J. H. Jiang, and M. Q. Weng, *Phys. Rep.* **493**, 61 (2010).
- [49] Y. G. Semenov, *Phys. Rev. B* **67**, 115319 (2003).
- [50] B. König, I. A. Merkulov, D. R. Yakovlev, W. Ossau, S. M. Ryabchenko, M. Kutrowski, T. Wojtowicz, G. Karczewski, and J. Kossut, *Phys. Rev. B* **61**, 16870 (2000).
- [51] Ł. Cywiński and L. J. Sham, *Phys. Rev. B* **76**, 045205 (2007).
- [52] E. Tsitsishvili and H. Kalt, *Phys. Rev. B* **73**, 195402 (2006).
- [53] R. J. Elliott, *Phys. Rev.* **96**, 266 (1954).
- [54] M. I. D'yakonov and V. I. Perel', *Zh. Eksp. Teor. Fiz.* **60**, 1954 (1971) [*Sov. Phys. JETP* **33**, 1053 (1971)].
- [55] F. Ungar, M. Cygorek, P. I. Tamborenea, and V. M. Axt, *Phys. Rev. B* **91**, 195201 (2015).
- [56] C. Thurn and V. M. Axt, *Phys. Rev. B* **85**, 165203 (2012).
- [57] M. Cygorek and V. M. Axt, *J. Phys.: Conf. Ser.* **647**, 012042 (2015).
- [58] C. Thurn, M. Cygorek, V. M. Axt, and T. Kuhn, *Phys. Rev. B* **87**, 205301 (2013).
- [59] M. Cygorek, P. I. Tamborenea, and V. M. Axt, *Phys. Rev. B* **93**, 035206 (2016); **94**, 079906(E) (2016).
- [60] M. Cygorek, F. Ungar, P. I. Tamborenea, and V. M. Axt, *Proc. SPIE* **9931**, 993147 (2016).
- [61] R. Bouzerar and G. Bouzerar, *Europhys. Lett.* **92**, 47006 (2010).
- [62] M. Cygorek, P. I. Tamborenea, and V. M. Axt, *Phys. Rev. B* **93**, 205201 (2016).
- [63] R. Kubo, *J. Phys. Soc. Jpn.* **17**, 1100 (1962).
- [64] F. Rossi and T. Kuhn, *Rev. Mod. Phys.* **74**, 895 (2002).
- [65] S. Butscher, J. Förstner, I. Waldmüller, and A. Knorr, *Phys. Rev. B* **72**, 045314 (2005).
- [66] M. Bonitz, J. W. Dufty, and C. Sub Kim, *Phys. Status Solidi B* **206**, 181 (1998).
- [67] M. Cygorek and V. M. Axt, *Semicond. Sci. Technol.* **30**, 085011 (2015).
- [68] M. Cygorek and V. M. Axt, *Phys. Rev. B* **90**, 035206 (2014).
- [69] C. Thurn, M. Cygorek, V. M. Axt, and T. Kuhn, *Phys. Rev. B* **88**, 161302(R) (2013).
- [70] G. Bastard, *Wave Mechanics Applied to Semiconductor Heterostructures*, Monographies de physique (Les Editions de Physique, JOUVE, France, 1990).
- [71] F. Long, W. E. Hagston, P. Harrison, and T. Stirner, *J. Appl. Phys.* **82**, 3414 (1997).
- [72] S.-K. Chang, A. V. Nurmikko, J.-W. Wu, L. A. Kolodziejski, and R. L. Gunshor, *Phys. Rev. B* **37**, 1191 (1988).
- [73] J. Schilp, T. Kuhn, and G. Mahler, *Phys. Rev. B* **50**, 5435 (1994).
- [74] C. Fürst, A. Leitenstorfer, A. Laubereau, and R. Zimmermann, *Phys. Rev. Lett.* **78**, 3733 (1997).